M Davis

CORNELL-SYDNEY UNIVERSITY ASTRONOMY CENTER
CORNELL UNIVERSITY
ITHACA, NEW YORK

June 1969

CSUAC 182

THEORY OF
POINT FED SPHERICAL REFLECTORS

J. J. Condon

I. INTRODUCTION

A feed antenna is called a point feed if its phase pattern is isotropic; that is, if the surfaces of constant phase of waves emitted by it are concentric spheres in its far field. Only a paraboloidal reflector can collimate the radiation from such a feed. A spherical reflector may be illuminated by a point feed only insofar as it approximates a paraboloid; otherwise the reflected, or secondary, pattern will deteriorate. In spite of this limitation, the simplicity and small size characteristic of point feeds make them attractive for use with spherical reflectors.

This report presents a theoretical analysis of point fed spherical reflectors. The variation of the secondary pattern with feed parameters, wavelength, and reflector dimensions is investigated. Finally formulas are given which permit the design of optimum point feeds for any spherical reflector and wavelength.

The course of the analysis is as follows. The two dimensional Fourier transform representation of the far field secondary pattern of a reflector antenna is written down in its most general form. The class of feed patterns considered is limited to those patterns which are rotationally symmetric, and the azimuthal integration is performed immediately. The remaining one dimensional integral is evaluated by two different methods. For the first, or "direct", method, single lobed rotationally symmetric cosine squared feed power

patterns are assumed. This class of patterns closely represents the patterns of practical simple feeds. The geometrical terms in the integral are evaluated exactly, and the resultant integration was performed numerically on a computer for a number of particular cases. The second, or "indirect" method of evaluation involves treating the spherical reflector as a paraboloidal reflector with phase errors. This method is valid only when the illuminated region of the spherical reflector being considered does not differ from the best fit paraboloidal reflector by more than a small fraction of a wavelength. The cases of greatest interest are not excluded by this requirement. Approximations are made for the phase errors introduced by spherical reflectors, and a simplified illumination pattern is assumed. With the introduction of a few dimensionless variables general formulas are derived relating antenna gain to values of feed parameters, reflector dimensions, and wavelength.

The last section is a summary which unifies the results obtained by the two methods of analysis. It also presents the results of the calculations in such a way that the reader may use them to design point feeds without having read the derivations.

II. DERIVATION OF THE PATTERN INTEGRAL

The far-field secondary pattern of a reflector type antenna is the two dimensional fourier transform of its aperture illumination (Kraus 1966, p. 167).

$$E(\phi) = \frac{1}{\lambda^2} \iint_{\text{aperture}} E(x,y)\exp\left(\frac{j2\pi\chi\sin\phi}{\lambda}\right)dxdy \qquad (1)$$

where $E(x,y)$ = magnitude of the illuminating field projected onto a plane above the reflector surface

χ = path length from feed to point of observation

ϕ = polar angle to the point of observation

λ = wavelength of the illuminating radiation

The reciprocity theorem (Kraus 1950, p. 252) states that the transmitting and receiving patterns of a given antenna are identical. However, the transmitting pattern is usually easier to imagine; and many standard terms, such as "illumination", are used in a way which implies transmission rather than reception. For these reasons, only transmitting patterns will be calculated in this report; but the results will apply to both transmission and reception.

Application of equation 1 to point fed spherical reflectors requires the introduction of a number of geometrical parameters which are shown in figure 1.

C = center of curvature of the spherical reflector

d = distance from the feed to a point on the reflector

F = location of the point feed

PP = parafocal point

R = spherical radius of the reflector

r = projected radius to a point on the reflector

r_m = projected radius of the reflector surface

z = feed distance below the parafocal point

θ = polar angle measured from the feed location

The location of an extended "point feed" is the center of its set of concentric equiphase spheres. The parafocal point is defined as the focal point of the paraboloid which best fits the sphere over the infinitesimal region below the feed. It is located a distance R/2 below the center of curvature.

For simplicity the illumination pattern of the feed is taken to be rotationally symmetric, so that $P = P(\theta)$ only. Then equation 1 (in polar coordinates r, ψ) can be integrated analytically over the coordinate ψ without any further information. It is clear from the symmetry of the problem that an optimum point feed must have a rotationally symmetric pattern anyhow, so that no cases of practical interest are lost through this restriction. We may now rewrite equation 1 in the polar coordinate form

$$E(\phi) = \frac{1}{\lambda^2}\int_0^{r_m} E(r)\exp\left(\frac{j2\pi}{\lambda}\epsilon(r)\right)\left[\int_0^{2\pi}\exp\left(\frac{j2\pi}{\lambda}\chi(r,\psi)\sin\phi\right)d\psi\right]rdr \qquad (2)$$

$\epsilon(r)$ is the path length error of a ray reflected from a

sphere. Figure 2 shows the geometry of the region over which the azimuthal integration is to be performed. We see that for a ring of radius r

$$\chi(r,\psi) = r\cos\psi \tag{3}$$

if we take $\chi(0,\psi) = 0$. Therefore the expression within the brackets of equation 2 is equal to

$$\int_0^{2\pi} \exp\left(\frac{j2\pi}{\lambda} r\cos\Psi\sin\phi\right)d\psi = \int_0^{2\pi} \cos\left(\frac{2\pi}{\lambda} r\cos\psi\sin\phi\right)d\psi + i\int_0^{2\pi} \sin\left(\frac{2\pi}{\lambda} r\cos\psi\sin\phi\right)d\psi \tag{4}$$

The second integral on the right side of equation 4 has an antisymmetric integrand over the interval $\psi = 0$ to $\psi = 2\pi$, so it vanishes. The remaining integral may be evaluated with the aid of the substitution:

$$u = \cos\psi, \quad du = -\sin\psi d\psi$$

Then

$$\int_0^{2\pi} \cos\left(\frac{2\pi}{\lambda} r\cos\psi\sin\phi\right)d\psi = 4\int_0^1 \frac{\cos\left(\frac{2\pi}{\lambda} r\sin\phi u\right)}{\sqrt{1-u^2}}\,du \tag{5}$$

From integral tables (Abramowitz and Stegun 1964, p. 360) we have the relation

$$J_\nu(z) = \frac{2\left(\frac{1}{2}z\right)^\nu}{\pi^{1/2}\Gamma\left(\nu+1/2\right)} \int_0^1 \left(1-t^2\right)^{\nu-1/2} \cos(zt)dt \tag{6}$$

Evaluation of equation 5 by equation 6 and substitution into equation 4 yields

$$\int_0^{2\pi} \exp\left(\frac{j2\pi}{\lambda} r\cos\Psi\sin\phi\right)d\Psi = 2\pi\, Jo\left(\frac{2\pi}{\lambda} r\sin\phi\right) \tag{7}$$

This relation may be substituted into equation 2 to give the pattern integral for a rotationally symmetric feed-reflector system.

$$E(\phi) = \frac{2\pi}{\lambda^2} \int_{o}^{r_m} E(r) \exp\left(\frac{j2\pi}{\lambda}\epsilon(r)\right) Jo\left(\frac{2\pi}{\lambda} r \sin\phi\right) rdr \quad (8)$$

III. DIRECT NUMERICAL EVALUATION OF THE PATTERN INTEGRAL FOR "COSINE SQUARED" POINT FEEDS

Two factors of equation 8 remain to be specified before the integration may be performed. The first, $E(r)$, depends on the exact form of the illumination power pattern, while the second, $\epsilon(r)$, depends only on the reflector and the location of the feed. These two factors are determined precisely in this section for cosine squared primary patterns, and an exact relation for the secondary polar power pattern $G(\phi)$ is derived. The relation has been evaluated numerically to provide the results presented in an earlier report (Condon, 1968). Polar patterns were also calculated for the AIO reflector at several frequencies and are presented here for the first time.

Let the normalized primary power pattern be

$$P(B,\theta) = \begin{cases} N(B)\cos^2(B\theta), & |B\theta| \leq \pi/2 \\ 0, & |B\theta| > \pi/2 \end{cases} \tag{9}$$

B is a parameter which controls the primary beamwidth, and N(B) is a normalizing factor defined by the condition

$$\int_{4\pi}\int P(B,\theta)\,d\Omega = 1 \tag{10}$$

The units of P are watts/steradian. Such a single lobed rotationally symmetric "cosine squared" power pattern is a good approximation to the power patterns of actual point feeds (dipoles and reflectors, yagis, helices, etc.). For this reason it is of practical value to make a precise numerical evaluation of equation 8 for cosine squared feed power

patterns. The form of the normalizing factor N(B) can be derived from its defining equation 10. We have

$$\int_0^{2\pi} \int_0^{\frac{\pi}{2B}} N(B) \cos^2(B\theta) \sin\theta \, d\theta \, d\Psi = 1 \qquad (11)$$

$$\int_0^{\frac{\pi}{2B}} \sin\theta \, [1 + \cos(2B\theta)] \, d\theta = \frac{1}{\pi N(B)}$$

$$\int_0^{\frac{\pi}{2B}} \sin\theta \cos(2B\theta) \, d\theta = \frac{1}{\pi N(B)} - [1 - \cos(\tfrac{\pi}{2B})] \qquad (12)$$

Integrating the left side of equation 12 by parts twice yields

$$\int_0^{\frac{\pi}{2B}} \sin\theta \cos(2B\theta) \, d\theta = \frac{\cos(\frac{\pi}{2B}) + 1}{1 - 4B^2} \qquad (13)$$

Substitution of equation 13 into equation 12 gives the desired result:

$$N(B) = \frac{1}{\pi\left[1 - \cos(\frac{\pi}{2B}) + \frac{\cos(\frac{\pi}{2B}) + 1}{1 - 4B^2}\right]} \qquad (14)$$

The value of the illuminating field upon reflection is

$$E(r) = \frac{\sqrt{P(B,\theta)}}{d(r)} \qquad (15)$$

where d(r) is the distance between the feed and the ring of radius r on the reflector.

The derivation of the size of the path error length, $\epsilon(r)$, introduced by a spherical reflector is a purely geometrical one. Figure 3 defines all the necessary geometrical parameters. The length of the path traveled by a ray emitted straight down from the feed and reflected up to the center of curvature of the reflector is $(R/2 - z) + R$. A ray which is emitted at an angle and which is reflected at a projected radius r must travel a distance $d + R \cos \alpha$ to reach the horizontal plane containing the center of curvature of the reflector. Thus the phase difference between the two rays will be

$$\frac{2\pi}{\lambda} \epsilon(r) = \frac{2\pi}{\lambda} \left[\left(\frac{R}{2} - z\right) + R - (d + R \cos \alpha) \right] \qquad (16)$$

from geometry we have

$$\cos \alpha, = \frac{\sqrt{R^2 - r^2}}{R}$$

and

$$\left(\frac{R}{2} + z + \sqrt{d^2 - r^2}\right)^2 + r^2 = R^2$$

so that

$$\sqrt{d^2 - r^2} = - \left(\frac{R}{2} + z\right) \pm \sqrt{R^2 - r^2} \qquad (17)$$

The positive sign of the radical in equation 17 must be chosen to insure that $\sqrt{d^2 - r^2}$ is positive.

$$d^2 = r^2 + \left(\frac{R}{2} + z\right)^2 + (R^2 - r^2) - 2\left(\frac{R}{2} + z\right) \sqrt{R^2 - r^2} \qquad (18)$$

Equation 18 is substituted into equation 16 to yield the phase error.

$$\frac{2\pi}{\lambda}\,\epsilon(r) = \frac{2\pi}{\lambda}\left[\frac{3R}{2} - z - \sqrt{R^2 - r^2} - \left\{R^2 + \left(\frac{R}{2} + z\right)\left[\left(\frac{R}{2} + z\right) - 2\sqrt{R^2 - r^2}\right]\right\}^{1/2}\right] \tag{19}$$

The result has been derived previously (Perona, 1966). One final geometrical result derivable from Figure 3 will prove useful, namely

$$\theta = \tan^{-1}\left(\frac{r}{\sqrt{R^2 - r^2} - \frac{R}{2} - z}\right) \tag{20}$$

Now we have enough information to evaluate equation 8. Since the feed illumination $P(\theta)$ has been normalized, we may obtain the secondary power gain pattern over an isotropic radiator $G(\Phi)$ from the relation.

$$G(\Phi) = |E(\Phi)|^2 \tag{21}$$

A computer program was written to make direct numerical evaluations of $G(\Phi)$. All of the relations that are used in the evaluations are listed in equation 22 below.

Equation 22:

$$G(\phi) = \left|\frac{2\pi}{\lambda^2}\int_0^{r_m}\frac{\sqrt{P}}{d}\,Jo\left(\frac{2\pi\, r\, \sin\phi}{\lambda}\right)\cos\left(\frac{2\pi\epsilon}{\lambda}\right) r\, d\, r\right|^2 + \left|\frac{2\pi}{\lambda^2}\int_0^{r_m}\frac{\sqrt{P}}{d}\,Jo\left(\frac{2\pi\, r\, \sin\phi}{\lambda}\right)\sin\left(\frac{2\pi\epsilon}{\lambda}\right) r\, d\, r\right|^2$$

(equations 8, 15, 21)

where

Forward Gain $G(o)$: $Jo = 1$

Beam width of feed
Radius of Curvature
Feed Position
Radius of reflector annulus

$$P(B,r,R,z) = \frac{\cos^2\left[B \tan^{-1} \left(\frac{r}{\sqrt{R^2 - r^2} - \frac{R}{2} - z} \right) \right]}{\pi \left[1 - \cos\left(\frac{\pi}{2B}\right) + \frac{\cos\left(\frac{\pi}{2B}\right) + 1}{1 - 4B^2} \right]}$$

(equations 9, 14, 20)

Phase error:

and $\frac{2\pi}{\lambda} \epsilon(r,R,z)$

$$= \frac{2\pi}{\lambda} \left[\frac{3R}{2} - z - \sqrt{R^2 - r^2} - \left\{ R^2 + \left(\frac{R}{2} + z\right) \left[\left(\frac{R}{2} + z\right) - 2\sqrt{R^2 - r^2} \right] \right\}^{1/2} \right]$$

(equation 19)

The Bessel functions $Jo(r,\phi,\lambda)$ were evaluated from the formulas (Abramowitz and Stegun 1964, p. 360 and p. 364)

$$Jo\left(\frac{2\pi\ r\ \sin\phi}{\lambda}\right) = \sum_{i=o}^{\infty} \frac{(-1)^i \left(\frac{\pi\ r\ \sin\phi}{\lambda}\right)^{2i}}{(i\ !)^2}, \quad \frac{2\pi}{\lambda} r \sin\phi \leq 2$$

$$Jo\left(\frac{2\pi\ r\ \sin\phi}{\lambda}\right) = \sqrt{\frac{\lambda}{\pi^2\ r\ \sin\phi}} \cos\left(\frac{2\pi\ r\ \sin\phi}{\lambda} - \frac{\pi}{4}\right), \quad \frac{2\pi}{\lambda} r \sin\phi \geq 2$$

Equation 22 was evaluated for a variety of frequencies and values of the feed parameters B and z for the Arecibo reflector (R = 265 m, r_m = 152 m). The variation of effective collecting area with the parameters B and z for the frequencies 74, 195, 430, 610, 960, and 1420 MHz was presented graphically in an earlier CSUAC report (Condon 1968). The values of B and z which maximize the collecting area of the Arecibo reflector were determined from these graphs; they obey the relations

3.7 cm (8.1 GHz)
HPBW = 19.°25
Gain = 18.54 db

$$z = 3.5\ \lambda^{1/2} \qquad \text{2.45 @ 611 MHz} \qquad \text{0.866 m @ 4880} \qquad (23)$$

$$B = 2.05\ \lambda^{-1/4} \qquad \text{2.77 @ 1 GHz} \qquad \text{2.45 @ 611 MHz} \qquad (24)$$

$$\text{HPBW} = \frac{\pi}{2B} = 0.766\ \lambda^{\frac{1}{4}} \text{ radians} = 43.^{\circ}9\ \lambda^{\frac{1}{4}}, = 21.^{\circ}86 \text{ @ } 4880 \text{ MHz}$$

$$G_{max} = \frac{4}{\quad} \qquad G_{dB} = 10 \log G_{max} \qquad = B = 4.12 \text{ @ } 4880 \text{ MHz}$$

where the lengths z and λ are expressed in meters. These optimum feed parameters were then used in the calculation of polar diagrams at the frequencies 74, 195, 327, 430, 611, 960, and 1420 MHz. (See figures 4-10.) All of the polar diagrams are similar to those of uniformly illuminated circular paraboloids of wavelength dependent diameters. The theoretical Arecibo antenna gain, beamwidth, position of the first null, and position and level of the first sidelobe are nearly the same as the corresponding parameters of a uniformly illuminated circular paraboloid of diameter

$$D = 149\ \lambda^{1/4}$$ 243 feet at 4880 MHz 382 feet at 1000 MHz $$186\ \lambda^{-\frac{1}{4}}$$ (NEROC Report (25)

where D and λ are expressed in meters. For example figure 11 presents the superimposed polar diagrams of a uniformly illuminated 149 meter (490 foot) diameter circular paraboloid and of the Arecibo antenna with an optimum cosine squared point feed at a frequency of 300 MHz (λ = 1 meter). There is a significant difference between the depths of the first nulls of the two curves of figure 11, the null of the pattern of the spherical reflector being rather shallow. This effect is caused by phase errors (Silver, 1949, p. 186) which are unavoidably associated with point fed spherical reflectors.

In preparation for the design of a feed for the 611 MHz multiple beam survey system (to be described in a later report), polar diagrams for the Arecibo reflector were calculated for a number of values of the feed parameters B and z at 611 MHz. Figure 12 shows the calculated variation of secondary beamwidth with the feed beamwidth parameter B for

five values of z. Those portions of the curves of figure 12 which are to the left of the broken line represent the performance of the antenna when the reflector is over-illuminated. The reflector may be considered "over-illuminated" when the illuminated region extends beyond the circle of rapidly changing phase error (see figure 18). Figure 12 shows that for a given value of z it is not possible to decrease the secondary beamwidth significantly by over-illumination. However, the beamwidth does depend on z, the distance of the feed below the parafocal point, since the radius of the circle defining the over-illumination region is proportional to $z^{1/2}$. Apparently the cosine of the phase angle of radiation reflected outside this circle changes so abruptly with radius (see figure 19), that the portion of the reflector outside the circle is effectively invisible to the feed.

Figure 13 shows the dependence of the first sidelobe level on the feed beamwidth parameter B for four values of z. Once again, the distance of the feed below the parafocal point is the more critical parameter. The feed beamwidth does effect the second sidelobe significantly, though. Figures 14 and 15 show the antenna diagrams at 611 MHz for z = 2.47 and B = 2.05 and B = 2.86 respectively.

Both B and z are important in the determination of the effective collecting area. Figures 16 and 17 present the variation of effective collecting area at 611 MHz with B and z respectively.

$\lambda = 0.4902\,m$

The results of the next section will show that the particular results presented here for the Arecibo reflector at 611 MHz may be scaled to apply to different reflectors and different frequencies.

IV. GENERALIZED INDIRECT EVALUATION OF THE PATTERN INTEGRAL BY THE PARABOLOIDAL APPROXIMATION METHOD

Although the direct, that is, "brute force," method of Section III for evaluating the far field pattern integral is capable of producing precise and useful numerical results for particular cases, it is too unwieldy to be generalized. Also, it does not present the functional dependence of $G(\phi)$ on the parameters B, z, λ, and R in a simple enough way that an intuitive understanding of the dependence is possible. It is therefore worthwhile to look for an approximation method which does not suffer from these two defects. One such method, which may be called the "paraboloidal approximation method," is presented in this section.

The shapes of a spherical reflector with radius of curvature R and of a paraboloidal reflector with focal length R/2 are very nearly identical over the regions which can be successfully illuminated by a point feed. Consequently, the only significant differences in antenna gain between a spherical and paraboloidal antenna arise from the phase errors associated with spherical reflectors. Even the phase errors are small. Numerical results of Section III indicate that the maximum path length error for a ray reflected from a point fed spherical reflector must be less than 0.2λ; $\equiv 72°$ otherwise the gain deteriorates badly. Thus one way to find the gain of a spherical antenna is to treat it as a paraboloidal antenna with phase errors. Such an approximation

method will be valid for all cases except those in which the phase errors become very large; that is, those cases in which the reflector is seriously over-illuminated.

In this section a polynomial expansion of the phase error introduced by a spherical reflector is derived. The phase error approximation is used to calculate the efficiency correction on the gain of a paraboloidal reflector of equal focal length, resulting in an expression for the gain G of the spherical antenna which shows clearly the dependence on B, z, λ, and R. It is assumed that the illumination does not spill over the edge of the reflector, so there is no dependence on r_m. The parameters B and z of feeds which maximize the gain are given in two simple formulas.

The path length error $\epsilon(r)$ of a ray reflected from a spherical reflector is (equation 19).

$$\epsilon(r) = \frac{3R}{2} - z\sqrt{R^2 - r^2} - \left\{R^2 + \left(\frac{R}{2} + z\right)\left[\left(\frac{R}{2} + z\right) - 2\sqrt{R^2 - r^2}\right]\right\}^{1/2}$$

Let r_o be defined as the value of r for which $|\epsilon|$ has a maximum. Then

$$\left.\frac{\partial|\epsilon|}{\partial r}\right|_{r=r_o} = 0 \qquad (26)$$

$$\frac{r_o}{\sqrt{R^2 - r^2}}\left[1 - \frac{\left(\frac{R}{2} + z\right)}{\left\{R^2 + \left(\frac{R}{2} + z\right)\left[\left(\frac{R}{2} + z\right) - 2\sqrt{R^2 - r_o^2}\right]\right\}^{1/2}}\right] = 0$$

$$r_o^2 = R^2 - \left(\frac{R^2}{R + 2z}\right)^2$$

This expression for r_o^2 may be rearranged to give

$$r_o^2 = 4Rz\left[\frac{1 + (\frac{z}{R})}{1 + 4(\frac{z}{R}) + 4(\frac{z}{r})^2}\right] \tag{27}$$

At this point it is convenient to define two dimensionless variables. The first is

$$\xi \equiv \frac{z}{R} \tag{28}$$

ξ is the ratio of the feed distance below the parafocal point to the spherical radius of the reflector. It will be small compared to one, so that we may approximate r_o^2 by expanding equation 27 to second order in ξ.

$$r_o^2 = 4Rz\left[1 - 3\xi + 0(\xi^2)\right] \tag{29}$$

The second dimensionless variable, k, is defined by the relation

$$k \equiv r/r_o \tag{30}$$

Using equations 29 and 30 we obtain the following expansion for the path error length ϵ.

$$\epsilon = R\left[\frac{3}{2} - \sqrt{1 - k^2 4\xi(1 - 3\xi)} - \xi - \left\{1 + (\frac{1}{2} + \xi)\left[\frac{1}{2} + \xi - 2\sqrt{1 - k^2 4\xi(1 - 3\xi)}\right]\right\}^{1/2}\right] + R \cdot 0(\xi^3) \tag{31}$$

We continue the expansion of equation 31 with the relation

$$\sqrt{1 - k^2 4\xi(1 - 3\xi)} = 1 - 2k^2\xi(1 - 3\xi) - 2(k^2\xi)^2 + 0(\xi^3)$$

so that

$$\epsilon = R\Big[\frac{1}{2} + (2k^2 - 1)\,\xi - (6k^2 - 2k^4)\,\xi^2 - \Big\{1 + \Big(\frac{1}{2} + \xi\Big)\Big[-\frac{3}{2} + (4k^2 + 1)\,\xi - 2\,(6k^2 - 2k^4)\,\xi^2\Big]\Big\}^{1/2}\Big] + R \cdot O\,(\xi^3) \qquad (32)$$

If a Taylor expansion to $O(\xi^3)$ of the square root term of equation 32 is made we obtain

$$\epsilon = R\Big[\frac{1}{2} - (2k^2 - 1)\,\xi - (6k^2 - 2k^4)\,\xi^2 - \frac{1}{2}\Big\{1 + 2\,(2k^2 - 1)\,\xi + 2\,(2k^4 - 2k^2 + 1)\,\xi^2 - 2\,(2k^2 - 1)^2\,\xi^2\Big\}\Big] + R \cdot O\,(\xi^3) \qquad (33)$$

Many of the terms of equation 33 cancel, leaving

$$\epsilon = -4R\xi^2\,(2k^2 - k^4) + R \cdot O\,(\xi^3) \qquad (34)$$

$\epsilon/(4R\xi^2)$ is plotted as a function of k in figure 18. Note the suddenness with which the path error increases for $k > 1.6$. If we substitute $k^2 = \left(\frac{r^2}{4Rz}\right)$ into equation 34 and multiply by $2\pi/\lambda$ we obtain the desired polynomial expansion of the phase error introduced by a spherical reflector.

$$\delta(r) = \frac{2\pi}{\lambda}\left(-\frac{2r^2 z}{R^2} + \frac{r^4}{4R^3}\right) \qquad (35)$$

The cosine of the phase error for optimum z (equation 23) is shown in Figure 19. If the illumination of the reflector extends beyond k = 1.6, the reflector is considered to be over-illuminated in the sense described in Section III.

The efficiency η of a paraboloidal reflector is related to the phase error distribution by (Ruze, 1966)

$$\eta = 1 - (\overline{\delta^2} - \overline{\delta}^2) \tag{36}$$

where

$$\overline{\delta^2} = \frac{\int_0^\infty f(r)\ \delta^2(r)\ r dr}{\int_0^\infty f(r)\ r dr}$$

$$\overline{\delta}^2 = \left[\frac{\int_0^\infty f(r)\ \ \delta(r)\ r dr}{\int_0^\infty f(r)\ r dr}\right]^2$$

$f(r)$ is the projected illumination power density on the reflector surface. The units of f are (watts/meter^2). Ideally $f(r)$ should represent the illumination of a cosine squared point feed. A compromise $f(r)$ ~~was chosen~~ was actually chosen so that subsequent integrations could be performed analytically. Let

$$f(r) = \left(\frac{1}{\gamma r_o}\right)^2 \left(1 - \frac{r}{\gamma r_o}\right), \quad o \leq r \leq \gamma r_o \tag{37}$$

$$f(r) = o \qquad\qquad , \ r > \gamma r_o$$

This is a linearly tapered illumination. γ is the illumination width parameter, and it may be related to the feed beamwidth parameter B through the condition that the ideal cosine squared illumination and the linearly tapered illumination vanish for the same value of r. For reasonably small θ we have then

$$\theta max = \frac{2\ r_{max}}{R}$$

so that

$$B = \frac{\pi R}{4r_{max}}$$

$$B = \frac{\pi}{8\gamma}\sqrt{\frac{R}{z}} \qquad (38)$$

When B and γ are related as in Equation 38, the linearly tapered illumination is a very good approximation to illumination from a cosine squared feed. See Figure 20 for a comparison of the two illumination tapers.

We now proceed to find η of equation 36. We assume that the illumination does not spill over the edge of the reflector, so that the upper limit of integration is $r = \gamma r_o$.

$$\overline{\delta^2} = \frac{\int_o^{\gamma r_o} \frac{1}{(\gamma r_o)^2}\left(1 - \frac{r}{\gamma r_o}\right)\frac{4\pi^2}{\lambda^2}\left(\frac{4rz}{R^4} + \frac{r^8}{16R^6} - \frac{r^6 z}{R^5}\right)rdr}{\int_o^{\gamma r_o} \frac{1}{(\gamma r_o)^2}\left(1 - \frac{r}{\gamma r_o}\right) rdr}$$

$$\overline{\delta^2} = \frac{4\pi^2}{\lambda^2}\left(\frac{12z^2\gamma^4 r_o^4}{21R^4} - \frac{z\gamma^6 r_o^6}{12R^5} + \frac{6\gamma^8 r_o^8}{1760R^6}\right) \qquad (39)$$

$$\overline{\delta^2} = \left[\frac{\int_o^{\gamma r_o} \frac{1}{(\gamma r_o)^2}\left(1 - \frac{r}{\gamma r_o}\right)\frac{2\pi}{\lambda}\left(-\frac{2r^2 z}{R^2} + \frac{r^4}{4R^3}\right) rdr}{\int_o^{\gamma r_o} \frac{1}{(\gamma r_o)^2}\left(1 - \frac{r}{\gamma r_o}\right) rdr}\right]^2$$

$$\overline{\delta^2} = \frac{4\pi^2}{\lambda^2}\left(\frac{9z^2\gamma^4 r_o^4}{25R^4} - \frac{3z\gamma^6 r_o^6}{70R^5} + \frac{\gamma^8 r_o^8}{784R^6}\right) \qquad (40)$$

Equations 39 and 40, with r_o^2 replaced by 4Rz, are now substituted into Equation 36.

$$\eta = 1 - 4\pi^2 \left(\frac{z^4}{R^2\lambda^2}\right)\left(\frac{592}{175}\gamma^4 - \frac{272}{105}\gamma^6 + \frac{1472}{2695}\gamma^8\right) \qquad (41)$$

A new dimensionless variable μ,

$$\mu \equiv \frac{z}{\sqrt{\lambda R}} \qquad (42)$$

is substituted in order to reach the final form of η, which contains only constants and dimensionless variables.

$$\eta = 1 - 4\pi^2\mu^4 \left(\frac{592}{175}\gamma^4 - \frac{272}{105}\gamma^6 + \frac{1472}{2695}\gamma^8\right) \qquad (43)$$

The effective collecting area A of a spherical reflector with a cosine squared feed is approximately equal to the product of the reflector efficiency η, the geometric illuminated area, and the aperture efficiency Q of a circular paraboloid with a cosine squared feed.

$$A = \eta\,(\pi\,\gamma^2\,r_o^{\,2})\,Q \qquad (44)$$

Q is defined by

$$Q = \left\{\frac{\left[\int_o^{\gamma r_o}\int_o^{2\pi}\sqrt{\cos^2\left(\frac{\pi}{2}\frac{r}{\gamma r_o}\right)}\;r\,d\Psi dr\right]^2}{\int_o^{\gamma r_o}\int_o^{2\pi}\cos^2\left(\frac{\pi}{2}\frac{r}{\gamma r_o}\right)\,r\,d\Psi dr}\right\} \Big/ (\pi\gamma^2\,r_o^{\,2})$$

Evaluation of equation 45 yields

$$Q = \frac{8}{\pi^2}\,\frac{\left[\frac{\pi}{2} - 1\right]^2}{\left[\frac{\pi^2}{16} - \frac{1}{4}\right]} = 0.72 \qquad (46)$$

If we replace $r_o^{\,2}$ by $4Rz$ in equation 43 and then substitute $\mu = z/\sqrt{\lambda R}$ we obtain

$$A = (4\pi Q)\,(\lambda^{1/2}\,R^{3/2})\,(\eta)\,(\gamma^2\mu) \qquad (47)$$

With the substitution of the right side of equation 43 for η, equation 47 becomes

$$A = (4\pi Q)\ (\lambda^{1/2}\ R^{3/2}) \left[\gamma_\mu^2 - 4\pi^2 \mu^5 \left(\frac{592}{175}\gamma^6 - \frac{272}{105}\gamma^8 + \frac{1472}{2695}\gamma^{10}\right)\right] \tag{48}$$

Equation 48 is the general equation for the collecting area of a spherical reflector with a cosine squared point feed. It is composed of just three factors. The first, $4\pi Q$, is just a number, 9.1. The second factor, $(\lambda^{1/2}\ R^{3/2})$, depends only on the wavelength and the spherical radius of the reflector. The third, in brackets, is purely dimensionless; and it can be maximized independently of the second. Therefore the maximum effective collecting area obtainable from a point fed spherical reflector is proportional to the square root of the wavelength and the 3/2 power of its spherical radius. Furthermore, the optimal values of γ and μ, which determine the feed parameters B and z, are the same for all reflectors and all wavelengths. We proceed by determining the values of γ and μ which maximize A by requiring that

$$\left(\frac{\partial A}{\partial \mu}\right)_\gamma = 0 \tag{49}$$

$$\left(\frac{\partial A}{\partial \gamma}\right)_\mu = 0$$

Application of the conditions of equation 49 to equation 48 results in the simultaneous algebraic equations below.

$$0 = 1 - 20\pi^2\mu^4 \left(\frac{592}{175}\gamma^4 - \frac{272}{105}\gamma^6 + \frac{1472}{2695}\gamma^8\right) \tag{50}$$

$$0 = 1 - 2\pi^2\mu^4 \left(\frac{3552}{175}\gamma^4 - \frac{2176}{105}\gamma^6 + \frac{2944}{539}\gamma^8\right)$$

The simultaneous solutions are

$$\gamma = 1.62 \tag{51}$$

$$\mu = 0.212$$

The optimal fundamental feed parameters B and z are determined by γ and μ through equations 38 and 42. Their values are

$$B = 0.52 \left(\frac{R}{\lambda}\right)^{1/4} \quad 2.84 @ 1 \text{ GHz} \tag{52}$$

$$z = 0.21 \left(R\lambda\right)^{1/2} \quad 6.19 \text{ ft} @ \text{ "} \tag{53}$$

If the optimal feed parameters are used, then the collecting area which can be obtained is

$$A = 4.1 \left(\lambda R^3\right)^{1/2} \tag{54}$$

The value of efficiency η is

$$\eta = 0.81 \quad A_e = 7855 \text{ m}^2 @ 1 \text{ GHz} \quad D_e = 100.00 \text{ m} @ 1 \text{ GHz} \tag{55}$$

Thus the phase errors introduced by an optimally point fed spherical antenna reduce its gain by about 0.9 db.

A generalized plot showing the variation of A with illuminated radius for various z and given λ and R can be made from equation 48. Figure 21 is such a plot; the abscissa $\gamma\mu^{1/2}$ is proportional to illuminated radius, and the parameter μ is proportional to z. The curve labeled "paraboloid" in Figure 21 was made by taking $\eta = 1$, in equation 48.

V. SUMMARY

The results of the two different methods of investigation just described compliment each other nicely. They can be used together to provide more information than both could provide separately. The direct method yields exact polar diagrams for specific cases, while the indirect method shows how the collecting area scales with the wavelength λ and reflector radius of curvature R. The direct method also provides verification of the accuracy of the indirect method, which involves several approximations. The dimensionless variables introduced in Section IV are used to derive formulas which are invariant under changes of λ and R, showing that the phase error distribution across the illuminated region of an optimally point fed spherical reflector is independent of λ and R (Figures 18 and 19). Therefore, we expect that the detailed polar diagrams of optimally point fed spherical antennas also scale, thus providing a justification for the concept of the "equivalent paraboloid" of equation 25 and permitting generalization of the qualitative discussion at the end of Section III about the variation of sidelobe level and secondary beam-width with the feed parameters.

The problem of designing the optimum cosine squared point feed (that is, the feed which maximizes the effective collecting area of the reflector) is considerably simplified by these scaling properties. Assuming a feed power pattern

$$P = N \cos^2 (B\theta)$$

where N is a normalizing factor, the two feed parameters which remain free are the feed beamwidth parameters B and the feed distance below the parafocal point z. (See Figure 1.) For a spherical reflector with radius of curvature R and for wavelength λ, the values of B and z which maximize the effective collecting area are

$$B = 0.52\left(\frac{R}{\lambda}\right)^{1/4}$$

$$z = 0.21\,(R\lambda)^{1/2}$$

These relations hold only when they do not suggest illumination beyond the edge of the reflector surface. They are valid for all frequencies above 70 MHz for the Arecibo reflector, for example. The effective collecting area of the reflector is then

$$A = 4.1\,(\lambda R^3)^{1/2}$$

The forward gain G over an isotropic radiator is related to the collecting area by

$$G = \frac{4\pi}{\lambda^2} A$$

The effective collecting area of the Arecibo antenna is usually described in terms of its sensitivity T, which is defined as the antenna temperature produced by a 1 flux unit source. If the effective area of the antenna is expressed in units of $(\text{meters})^2$, then

$$T = 3.62 \cdot 10^{-4} A \quad {}^{\circ}\text{K/flux unit} \qquad (56)$$

The secondary pattern of a spherical reflector with the optimum cosine squared point feed is very similar to that of a uniformly illuminated paraboloidal reflector with projected diameter D where

$$D = 2.26\,(\lambda R^3)^{1/4}$$

The effects of deviation from the optimum feed parameters cannot be described so simply. An earlier report (Condon 1968) shows the dependence of effective collecting area on the feed parameters for the Arecibo reflector at several frequencies. Over-illumination (too small a value of B) results in almost no narrowing of secondary beamwidth unless z is simultaneously increased. The sidelobe level depends primarily on z. For examples of these effects, see Figures 12 and 13.

ACKNOWLEDGEMENTS

The author would like to thank Professor C. Hazard for suggesting this investigation and for his helpful advice.

The Arecibo Ionospheric Observatory is operated by Cornell University with the support of the Advanced Research Projects Agency and the National Science Foundation under contract with the Air Force Office of Science Research.

FIGURE CAPTIONS

Figure 1 -- Geometrical parameters of a point fed spherical antenna

Figure 2 -- Integration over the azimuthal coordinate Ψ

Figure 3 -- Path length of a ray reflected from a sphere

Figure 4 -- Abscissa: Polar angle ϕ (degrees)
Ordinate: Gain (decibels)
Parameter: Frequency = 74 MHz

Figure 5 -- Abscissa: Polar angle ϕ (degrees)
Ordinate: Gain (decibels)
Parameter: Frequency = 195 MHz

Figure 6 -- Abscissa: Polar angle ϕ (degrees)
Ordinate: Gain (decibels)
Parameter: Frequency = 327 MHz

Figure 7 -- Abscissa: Polar angle ϕ (minutes)
Ordinate: Gain (decibels)
Parameter: Frequency = 430 MHz

Figure 8 -- Abscissa: Polar angle ϕ (minutes)
Ordinate: Gain (decibels)
Parameter: Frequency = 611 MHz

Figure 9 -- Abscissa: Polar angle ϕ (minutes)
Ordinate: Gain (decibels)
Parameter: Frequency = 960 MHz

Figure 10 -- Abscissa: Polar angle ϕ (minutes)
Ordinate: Gain (decibels)
Parameter: Frequency = 1420 MHz

Figure 11 -- Abscissa: Polar angle ϕ (minutes)
Ordinate: Gain (decibels)
Parameters: Frequency = 300 MHz
spherical reflector,
paraboloidal reflector

Figure 12 -- Abscissa: Feed beamwidth parameter B
Ordinate: Half-power beam width (minutes)
Parameters: Feed distance z below the
parafocal point (meters)
Frequency = 611 MHz

Figure 13 -- Abscissa: Feed beamwidth parameter B
Ordinate: Level of first sidelobe relative
to main beam (decibels)
Parameters: Feed distance z below the
parafocal point (meters)
Frequency = 611 MHz

Figure 14 -- Abscissa: Polar angle ϕ (minutes)
Ordinate: Gain (decibels)
Frequency : 611MHz

Figure 15 -- Abscissa: Polar angle ϕ (minutes)

Ordinate: Gain (decibels)

Frequency: 611 MHz

Figure 16 -- Abscissa: Feed beamwidth parameter B

Ordinate: Effective collecting area (1 unit = 10^4 M^2)

Parameter: Feed distance z below the parafocal point (meters)

Figure 17 -- Abscissa: Feed distance z below the prafocal point (meters)

Ordinate: Effective collecting area (1 unit = 10^4 M^2)

Parameter: Feed beamwidth parameter B

Figure 18 -- Abscissa: Dimensionless radius k

Ordinate: Dimensionless path length error $\epsilon/(4R\ \xi^2)$

Figure 19 -- Abscissa: Dimensionless radius k

Ordinate: Cosine of reflector phase error for optimal feed location

Figure 20 -- Abscissa: Dimensionless radius k

Ordinate: Relative power

Parameters: P = power of cosine squared feed

F = power of linearly tapered feed

Figure 21 -- Abscissa: Dimensionless radius $\gamma\mu^{1/2}$

Ordinate: Dimensionless effective area

$A_{eff} / (\lambda^{1/2} R^{3/2})$

Parameter: Dimensionless feed distance below parafocal point μ.

DICTIONARY OF VARIABLES

Name	Description	Defining Equation or Figure
A	antenna effective collecting area	
B	feed beamwidth parameter	Equation 9
C	spherical reflector center of curvature	Figure 1
D	diameter of the "equivalent paraboloid"	Equation 25
d	distance from feed to a point on the reflector	Figure 1
E	magnitude of electric field vector	
F	feed location	Figure 1
f	linearly tapered reflector illumination pattern	Equation 37
G	power gain over an isotropic radiator	
J_o	zeroth order Bessel function	
k	dimensionless radius	Equation 30
N	Cosine squared feed power normalization factor	Equation 10
P	feed pattern, power per unit solid angle	Equation 9
PP	parafocal point	Figure 1
Q	aperture efficiency of a circular paraboloid with cosine squared illumination	Equation 45
R	spherical radius of the reflector	Figure 1
r	projected radius to a point on the reflector	Figure 1

Name	Description	Defining Equation or Figure
r_m	projected radius of the reflector surface	Figure 1
r_o	projected radius with maximum phase error	Equation 26
T	antenna sensitivity in degrees per flux unit	Equation 56
z	feed distance below the parafocal point	Figure 1
α	angle between the vertical and a line segment connecting the spherical center and a point of the reflector	Figure 3
γ	reflector illumination width parameter	Equation 37
δ	polynomial approximation of phase error due to reflection from a sphere	Equation 35
ϵ	path error length due to reflection from a sphere	Equation 16
η	reflector efficiency	Equation 36
θ	polar angle measured from feed location	Figure 1
λ	wavelength	
μ	dimensionless feed distance below the parafocal point	Equation 42
ξ	dimensionless feed distance below the parafocal point	Equation 28
ϕ	polar angle from reflector normal to point of observation	Figure 2 Equation 1
χ	path length from feed to point of observation	Equation 1
Ψ	azimuth angle	Figure 2

REFERENCES

Abramowitz and Stegun (1964). Handbook of Mathematical Functions. (U.S. Government Printing Office, Washington, D.C.)

Condon (1968). "Cosine Squared" Point Feeds for the Arecibo Reflector. (CSUAC 126)

Kraus (1950). Antennas. (McGraw-Hill: New York)

Kraus (1966). Radio Astronomy. (McGraw-Hill: New York)

Perona (1966). A Correcting Feed at 611 MHz for the AIO Reflector. (CRSR 224)

Ruze (1966). Proc. IEEE, 54, 633.

Silver, S. (1949). Microwave Antenna Theory and Design. (McGraw-Hill: New York).

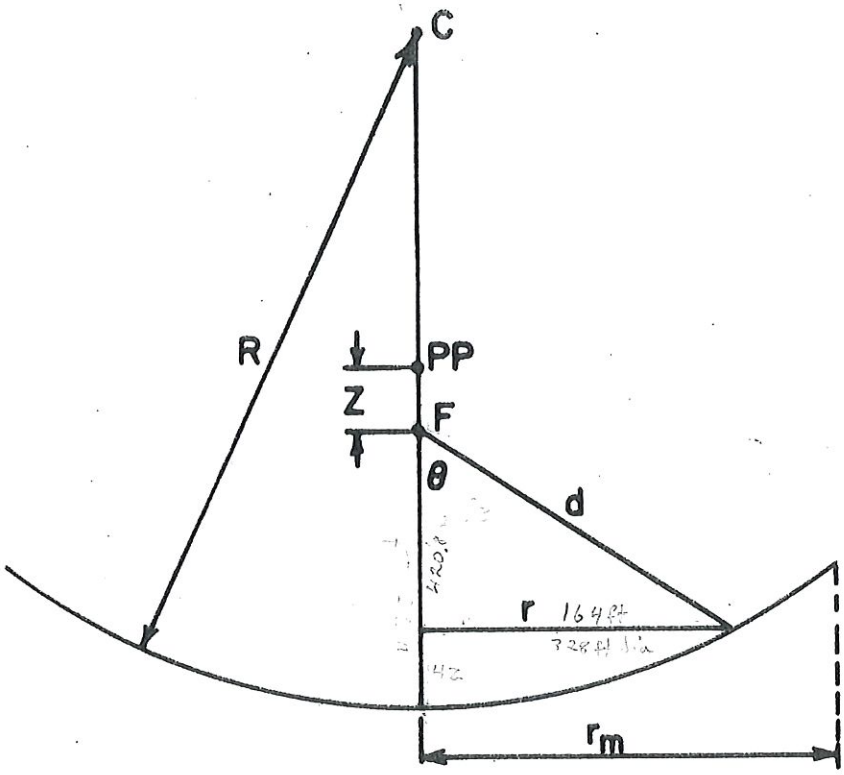

Figure 1

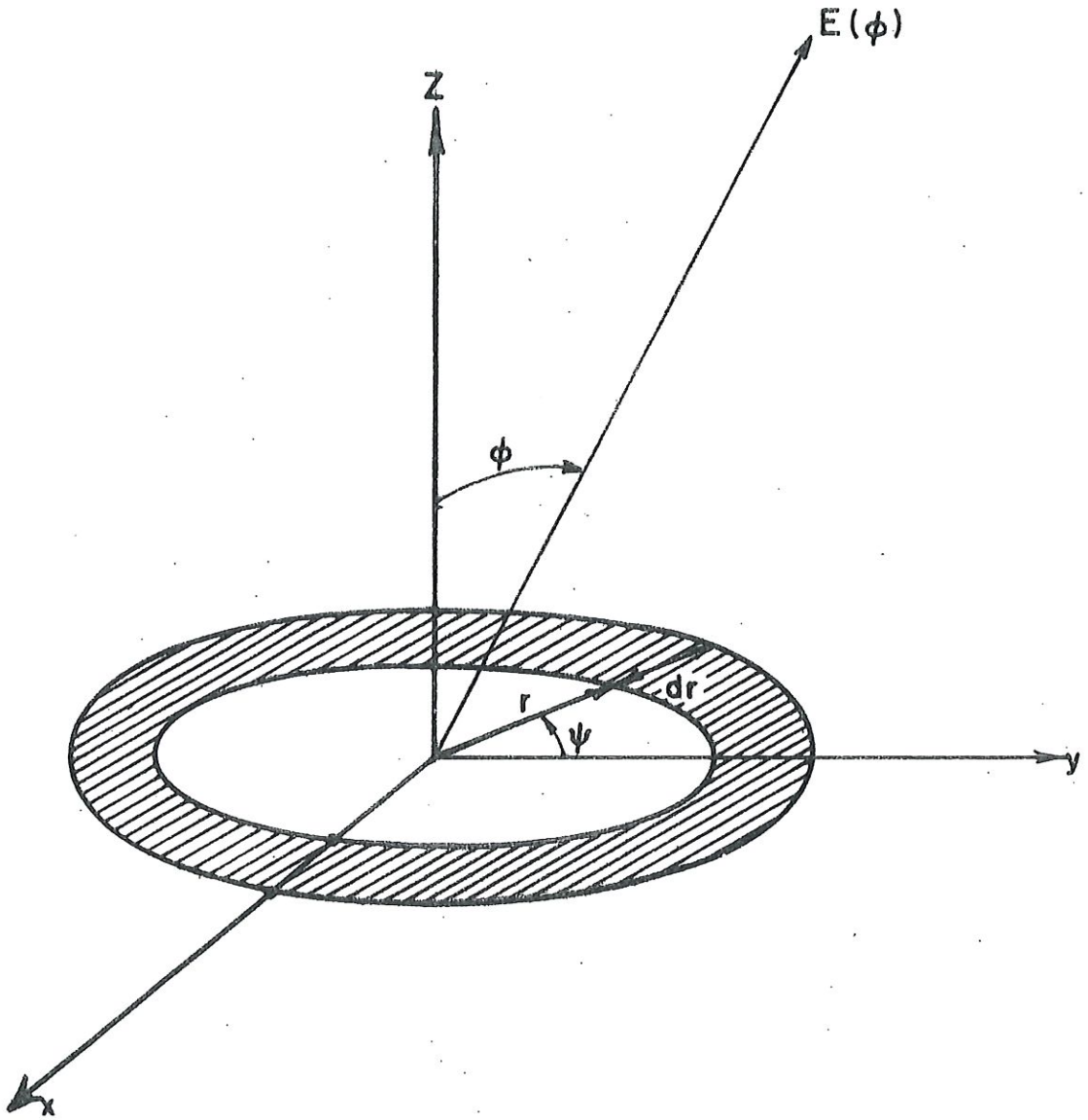

Figure 2

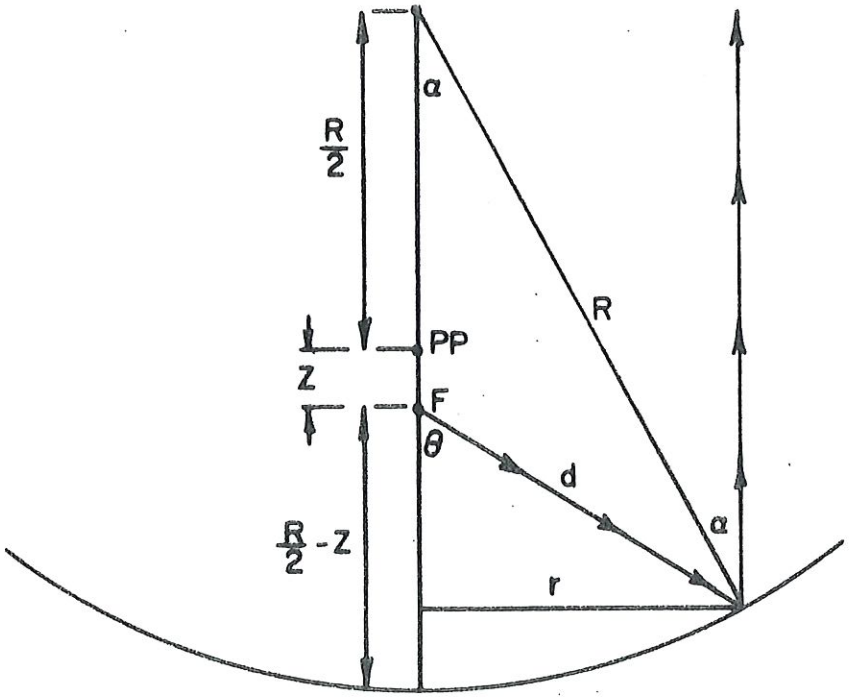

Figure 3

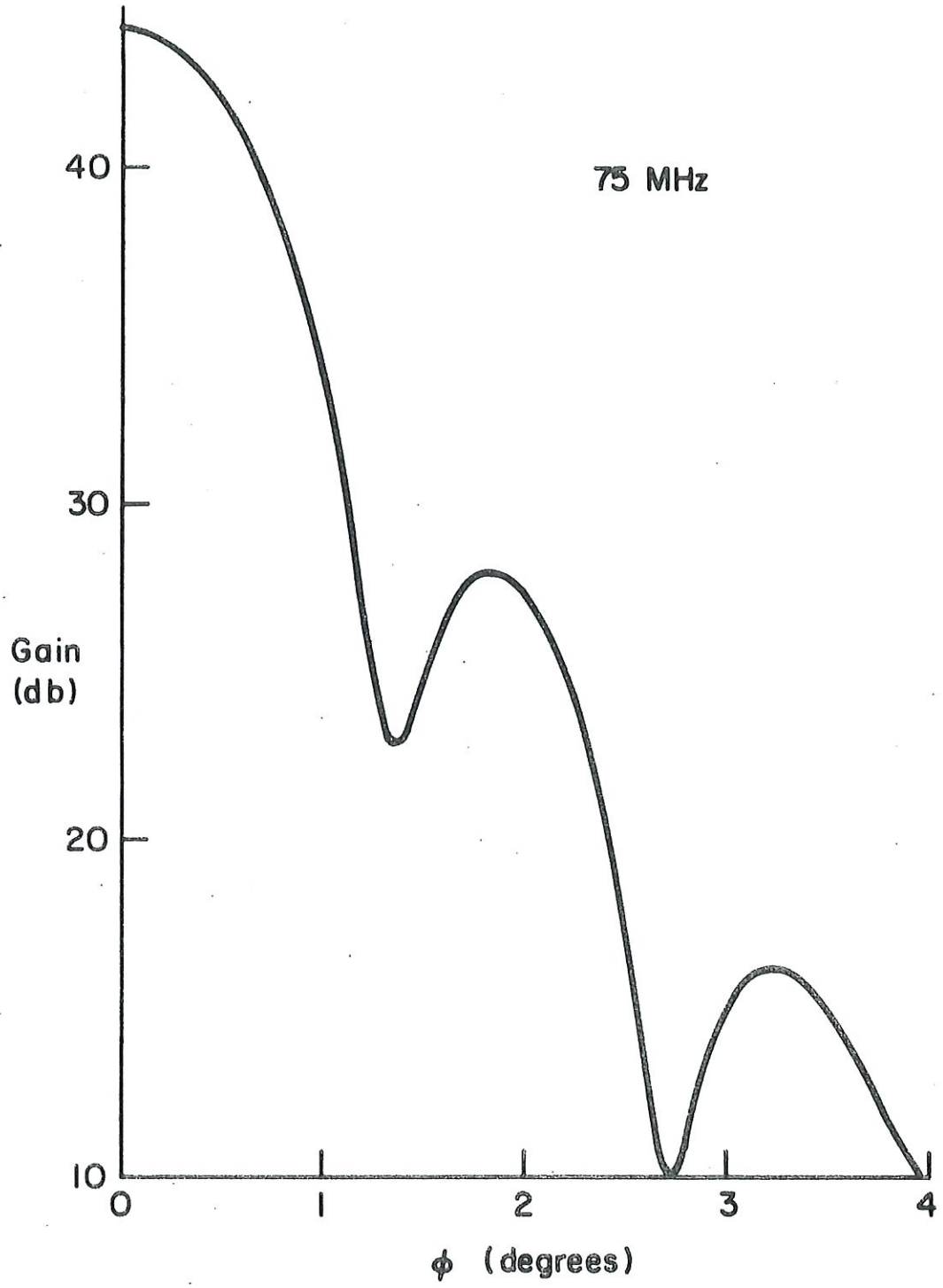

Figure 4

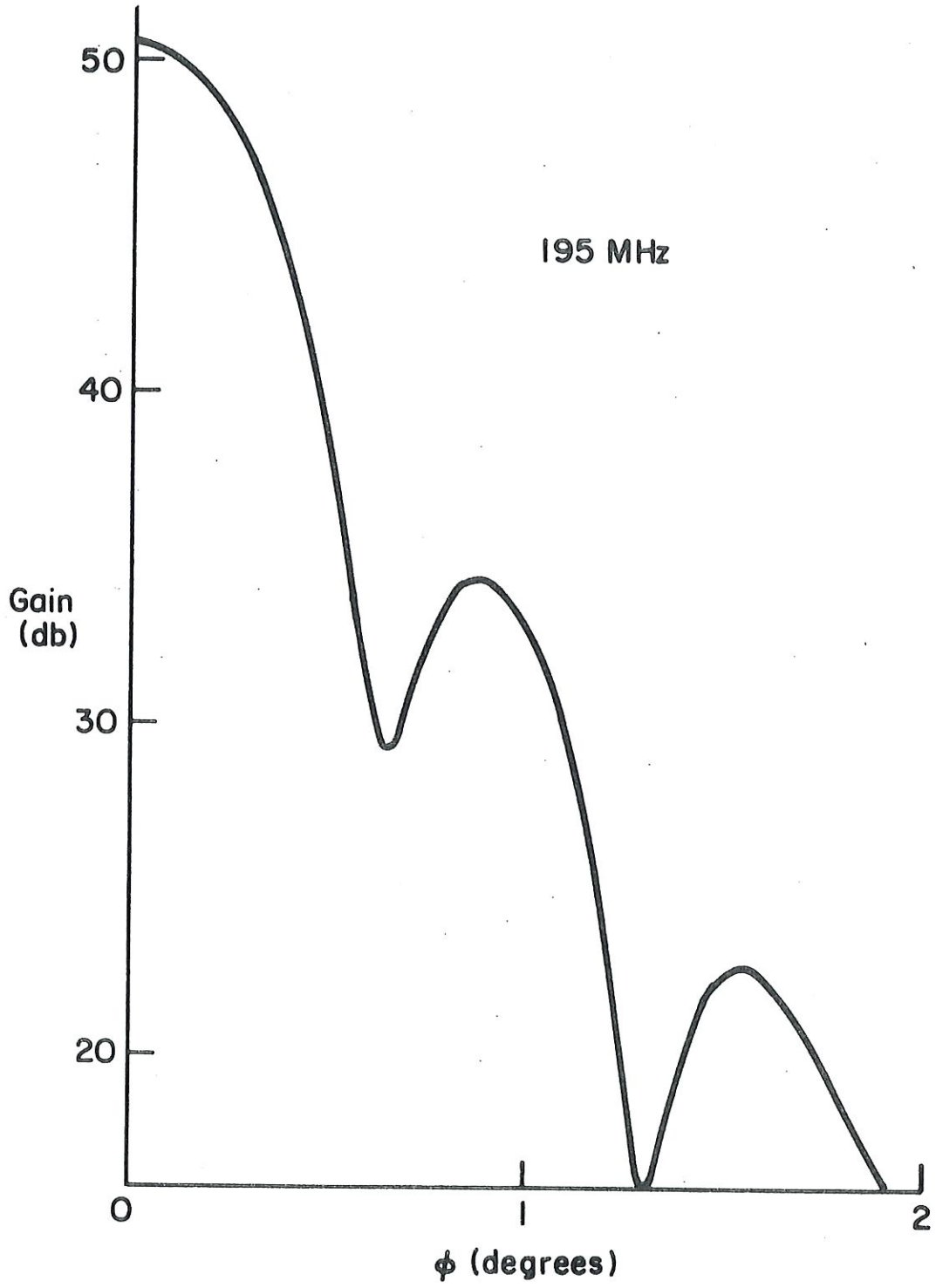

Figure 5

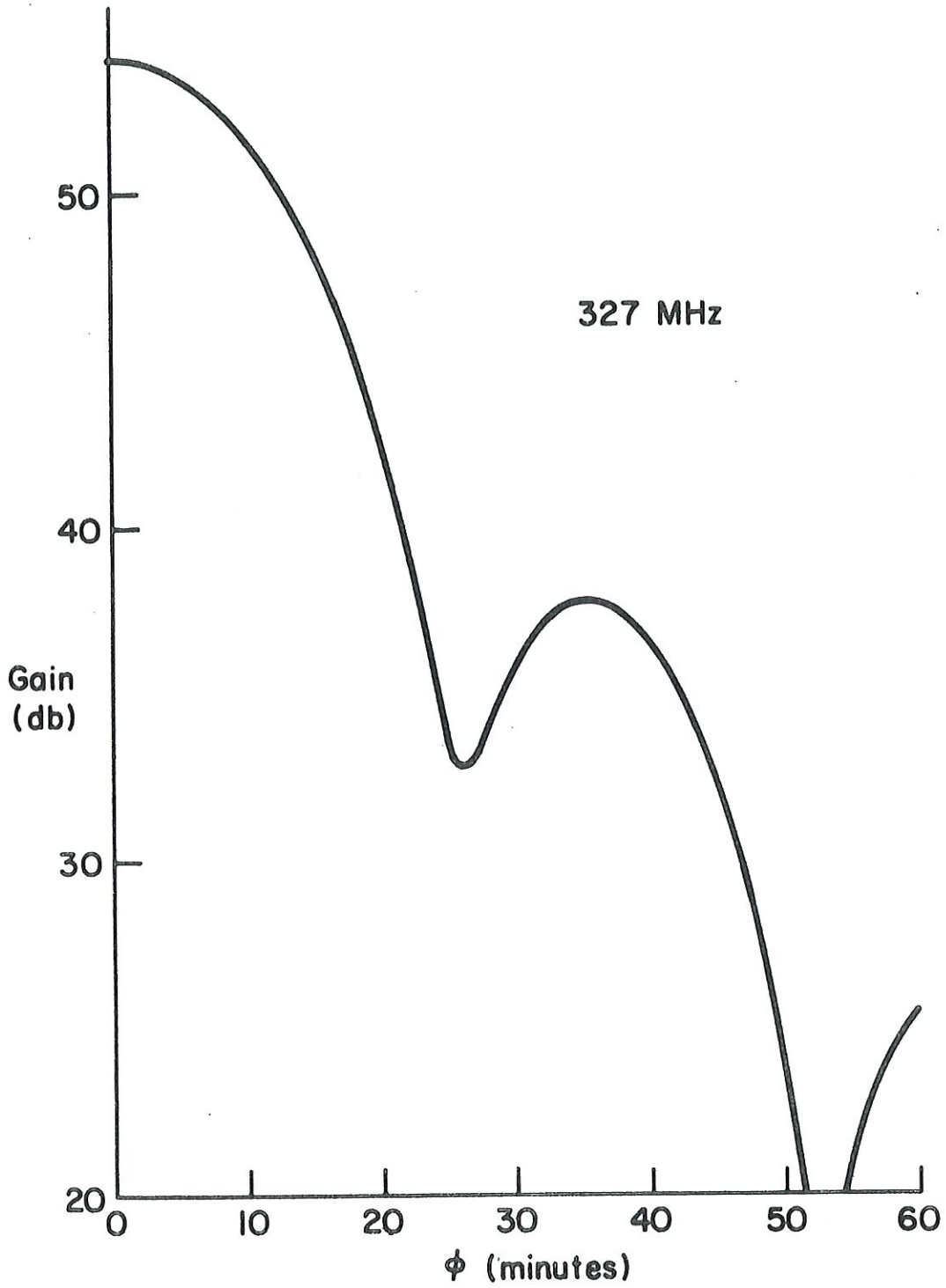

Figure 6

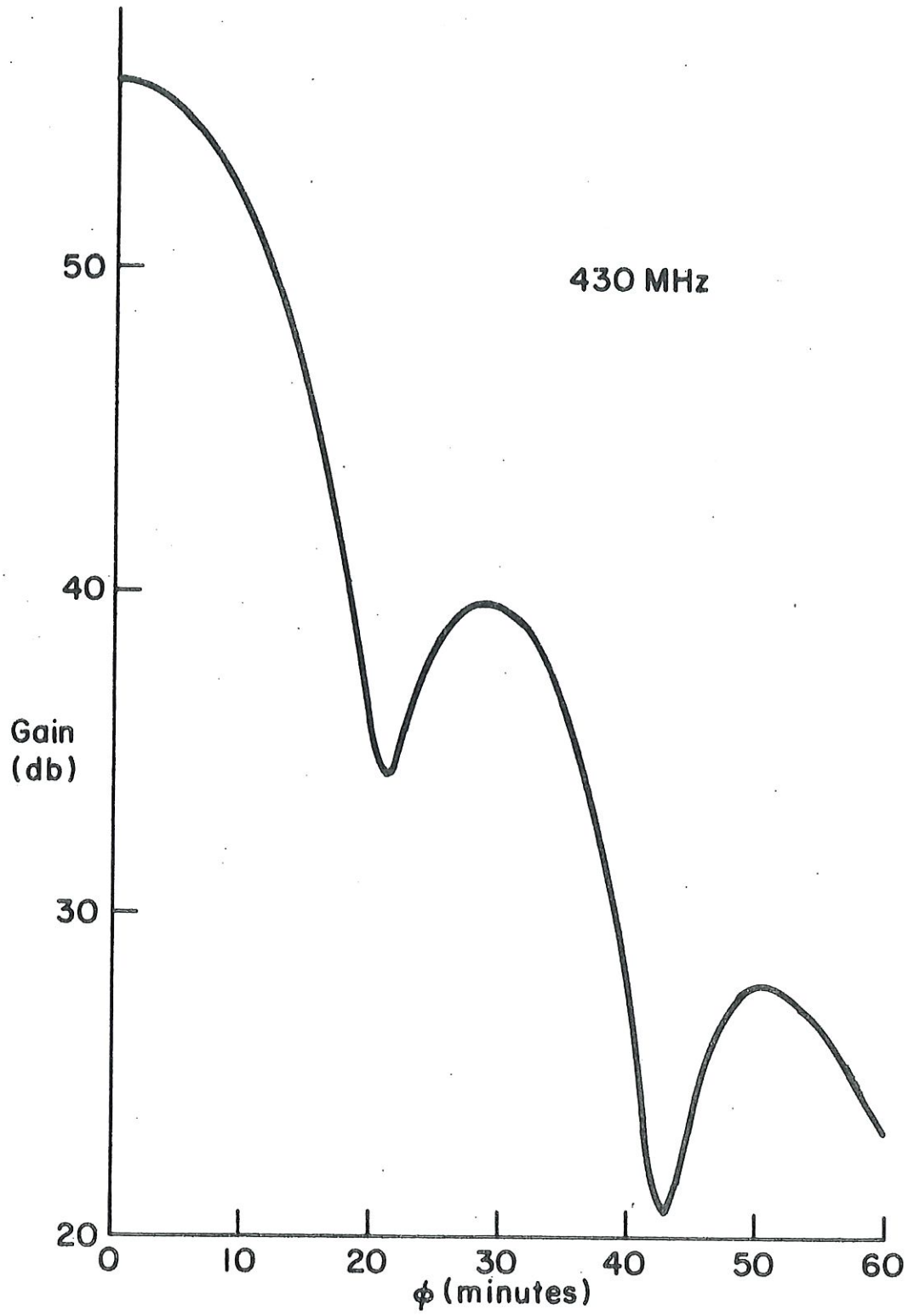

Figure 7

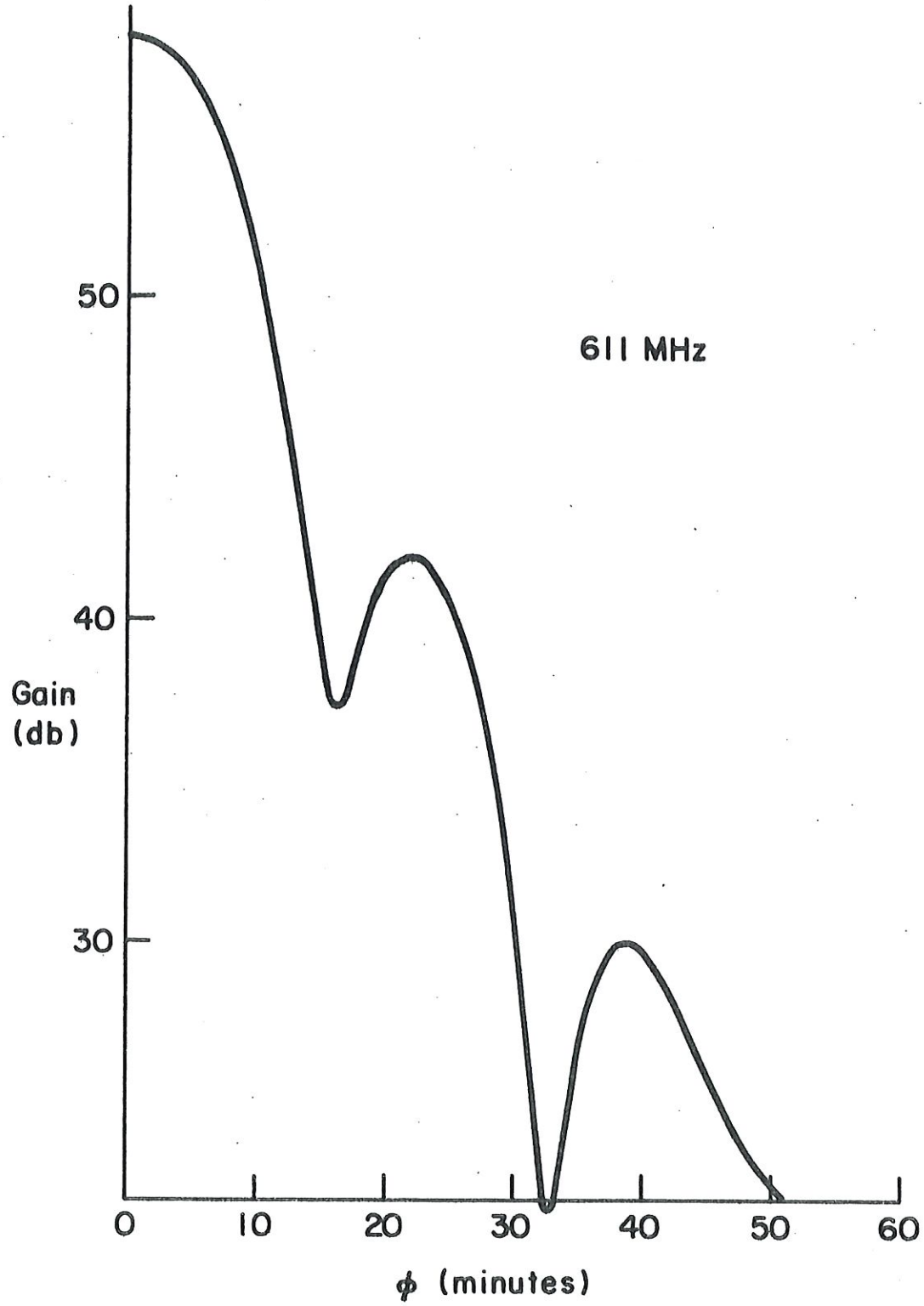

Figure 8

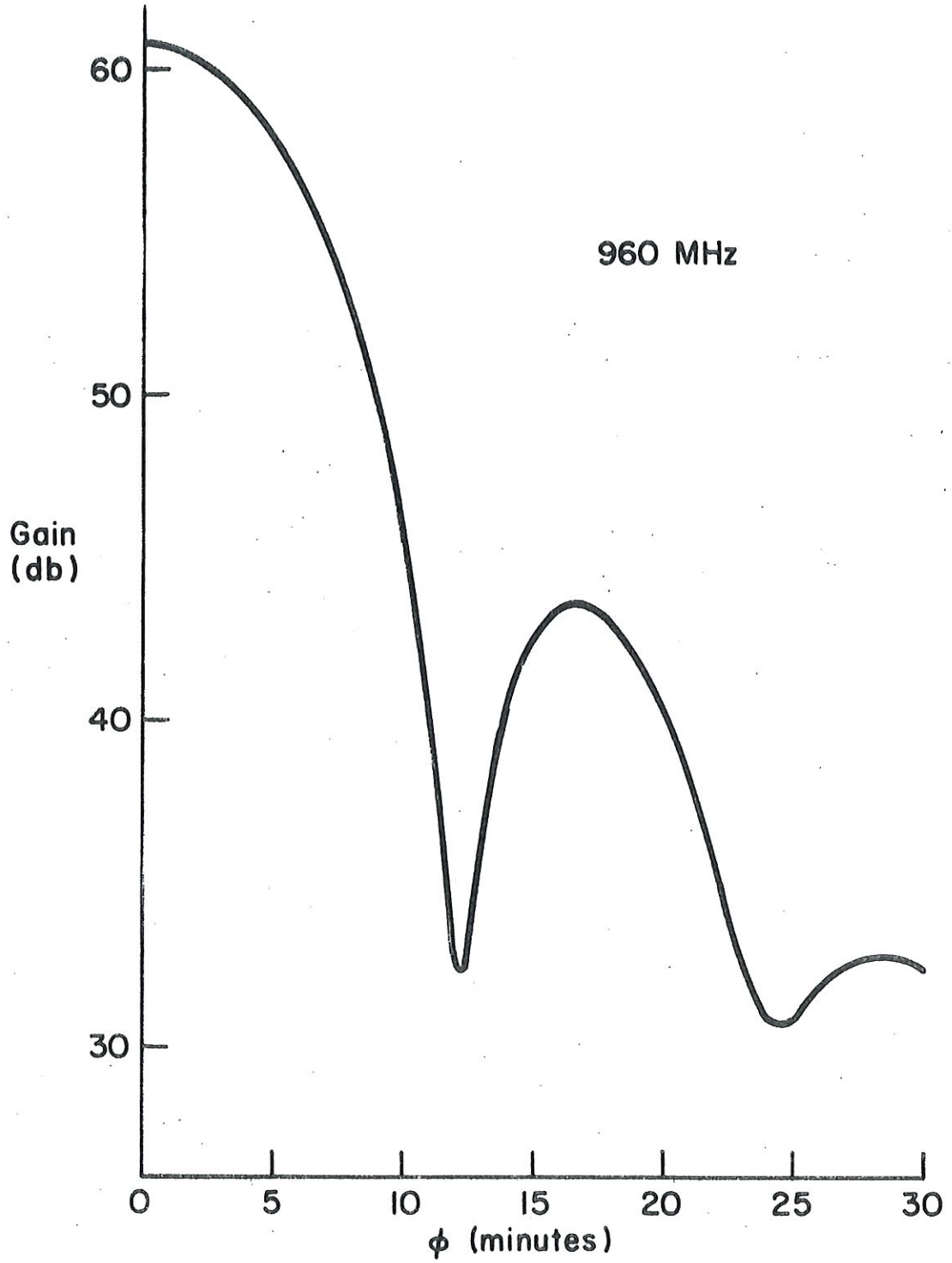

Figure 9

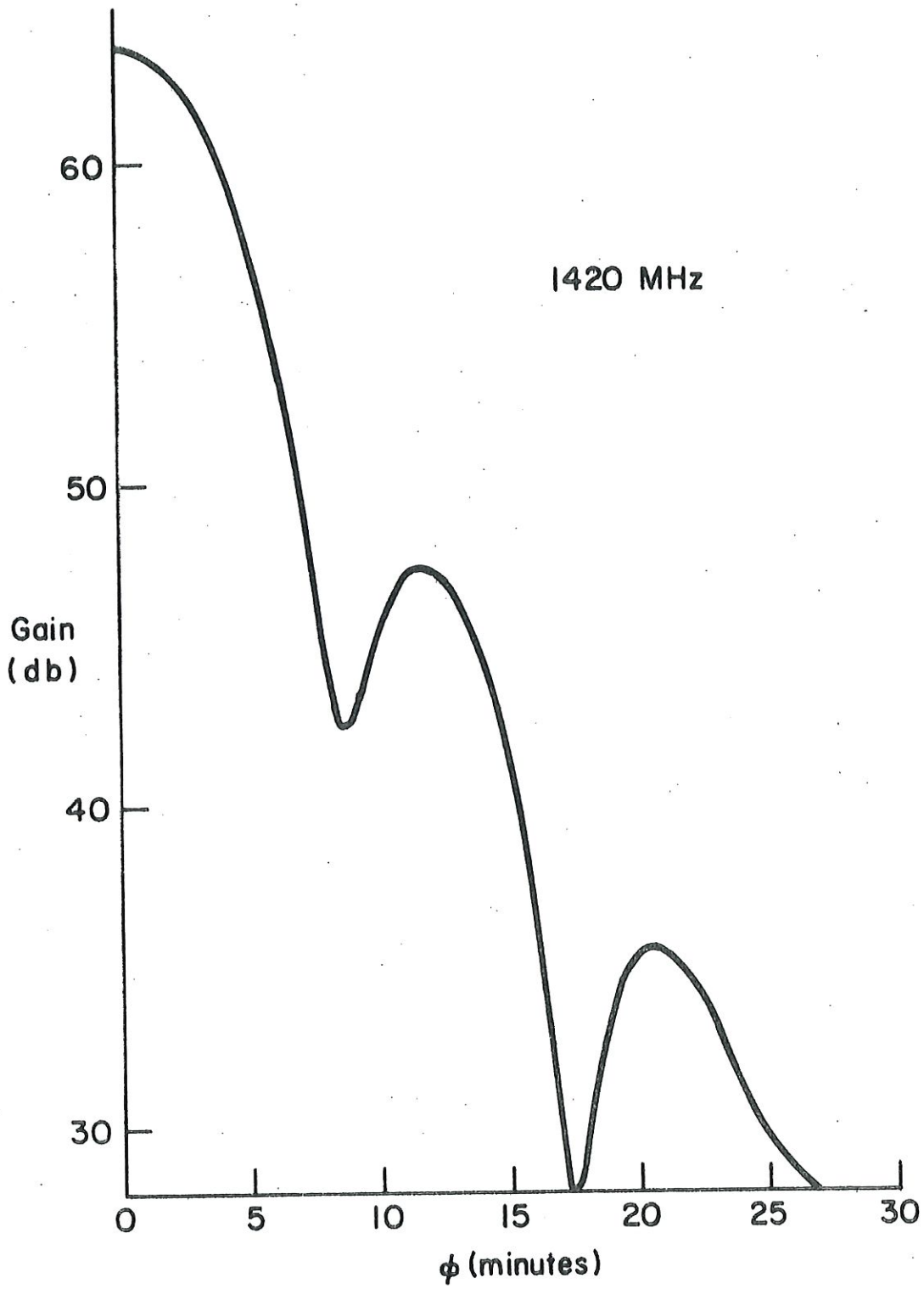

Figure 10

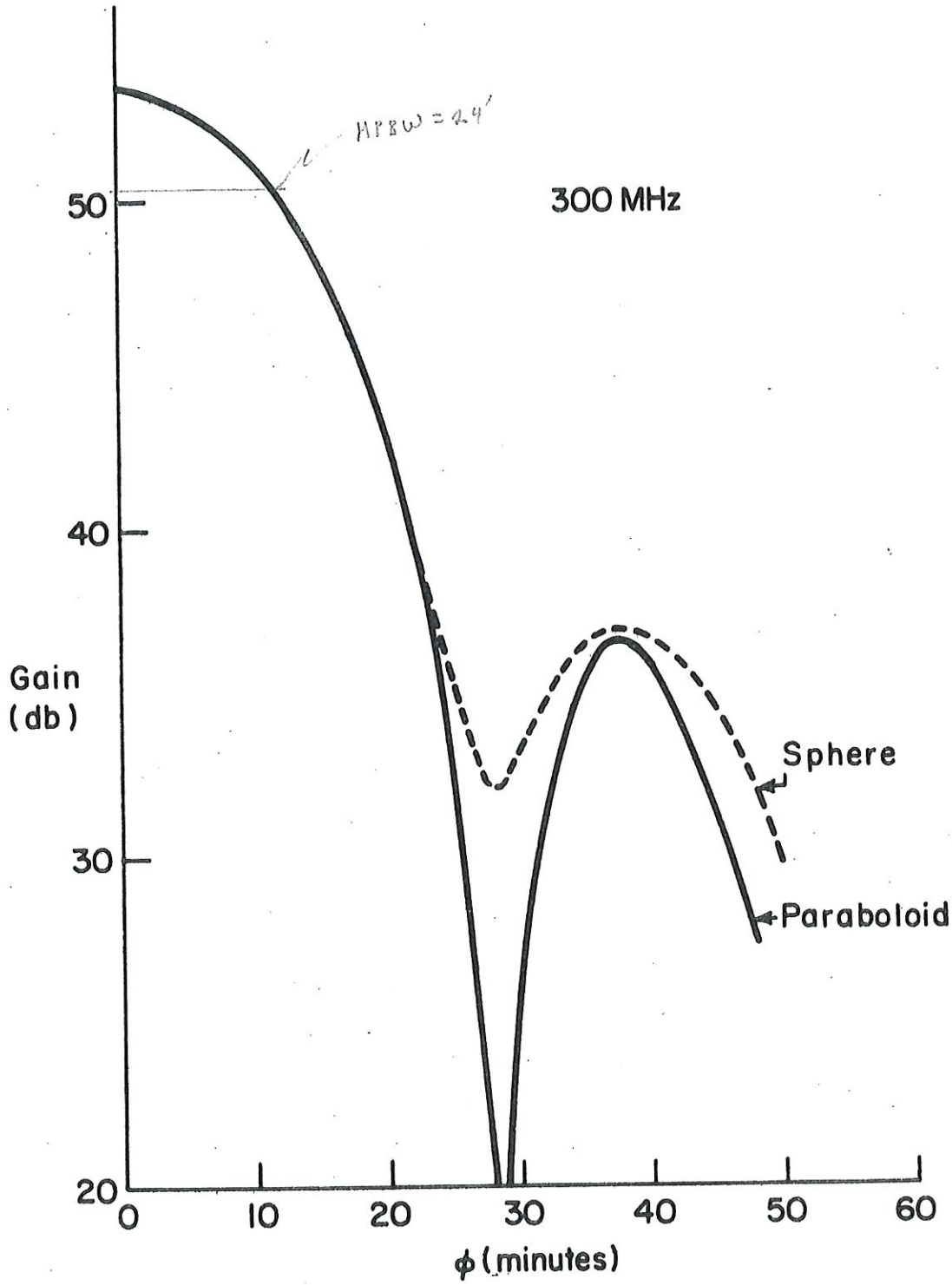
HPBW = 2.4'
300 MHz
50
40
30
20
Gain
(db)
Sphere
Paraboloid
0
10
20
30
40
50
60
φ (minutes)

Figure 11

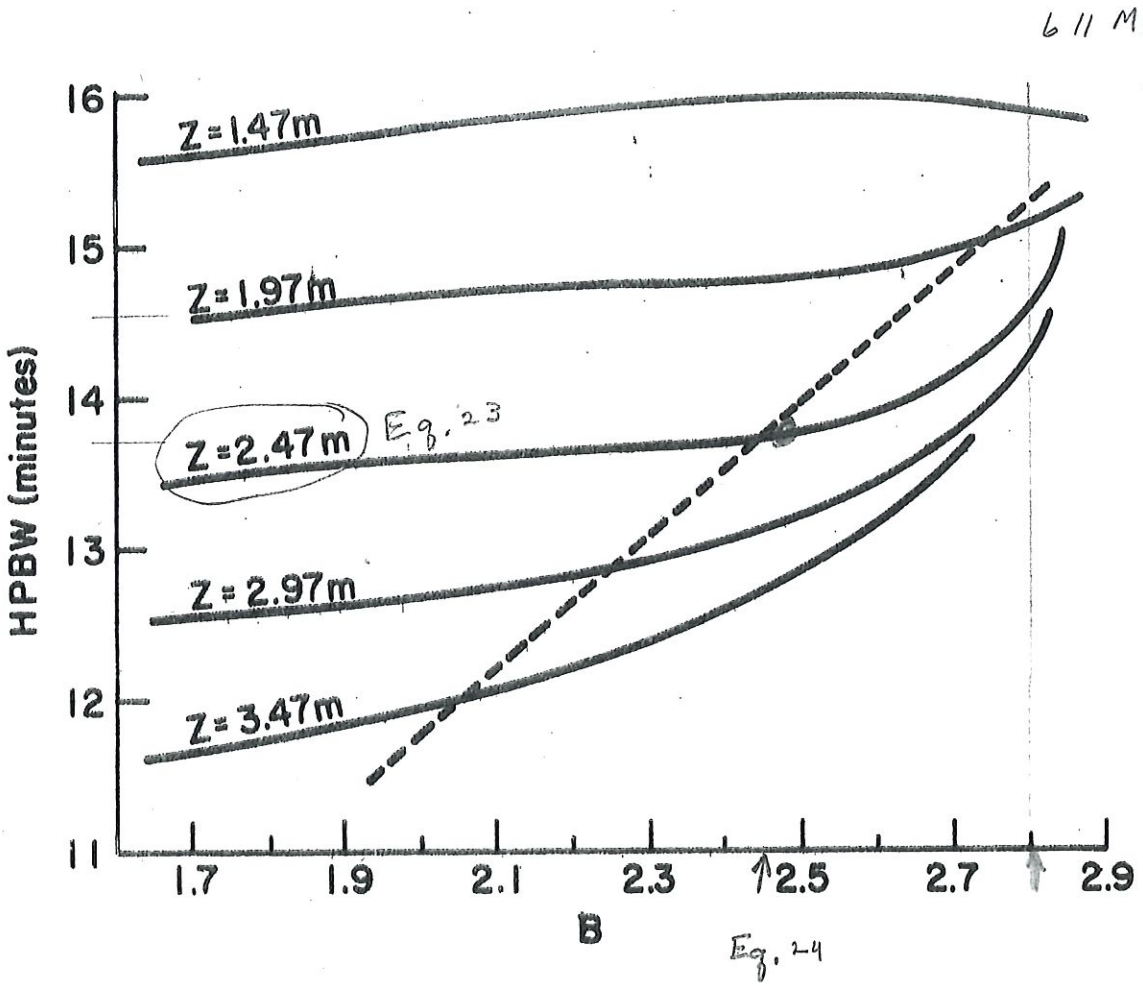
6 11 MHz
16
15
14
13
12
11
HPBW (minutes)
Z = 1.47m
Z = 1.97m
Z = 2.47m
Eq. 23
Z = 2.97m
Z = 3.47m
1.7
1.9
2.1
2.3
2.5
2.7
2.9
B
Eq. 24

Figure 12

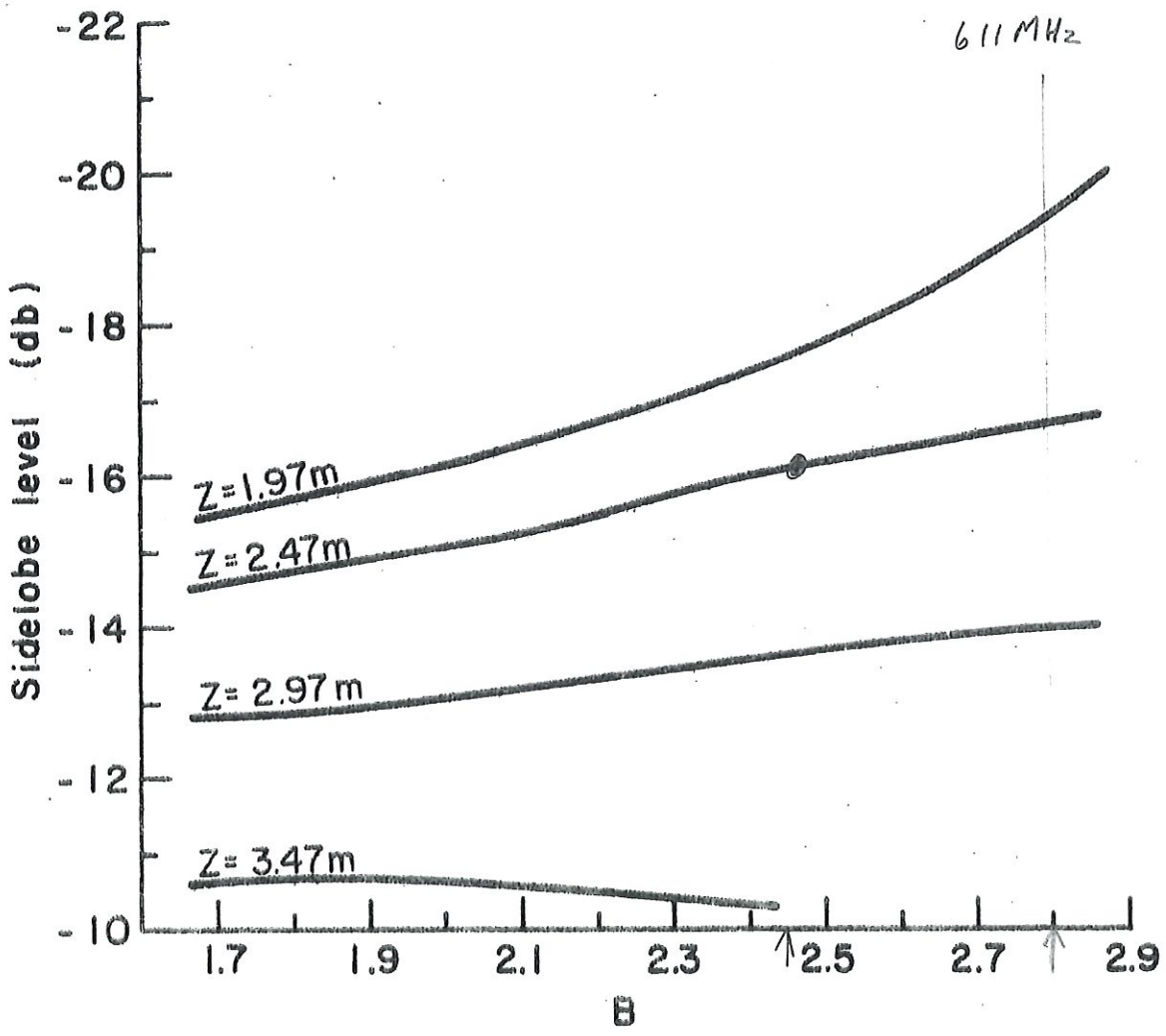
611 MHz
-22
-20
-18
-16
-14
-12
-10
Sidelobe level (db)
Z=1.97m
Z=2.47m
Z=2.97m
Z=3.47m
1.7
1.9
2.1
2.3
2.5
2.7
2.9
B

Figure 13

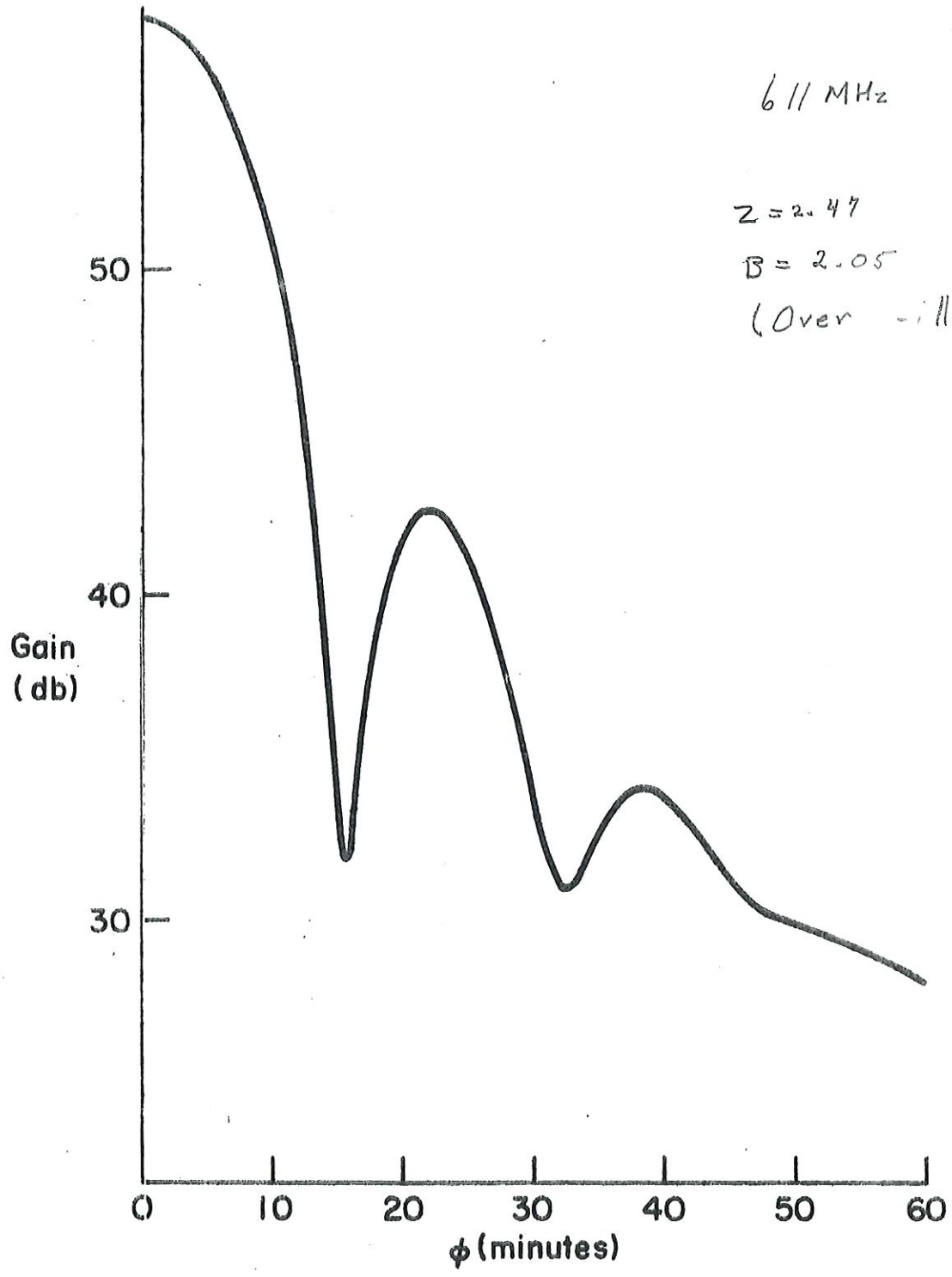
611 MHz
Z = 2.47
B = 2.05
(Over - illuminated)
50
40
30
Gain
(db)
0
10
20
30
40
50
60
φ (minutes)

Figure 14

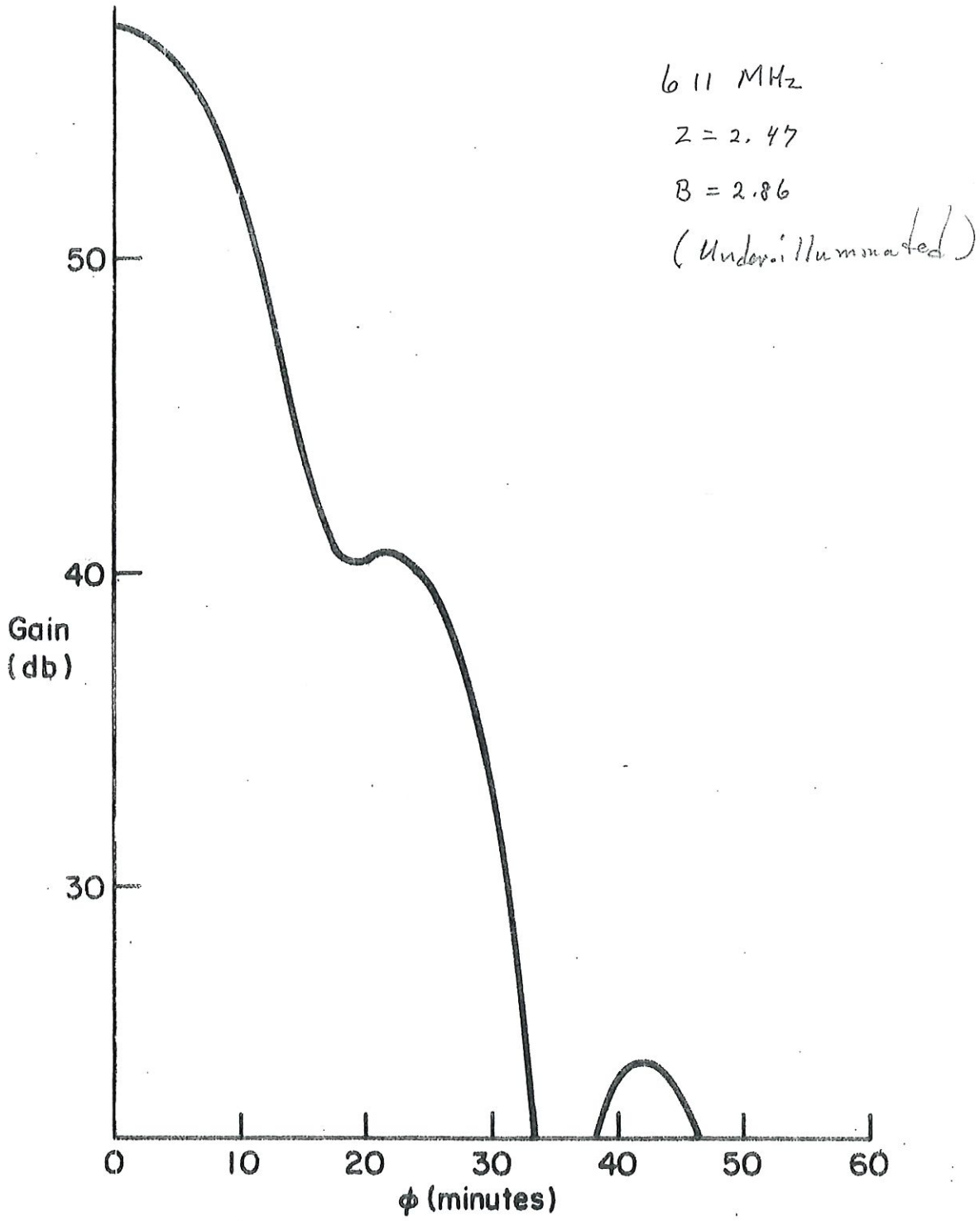
611 MHz
Z = 2.47
B = 2.86
(Underilluminated)
50
40
30
Gain
(db)
0
10
20
30
40
50
60
φ (minutes)

Figure 15

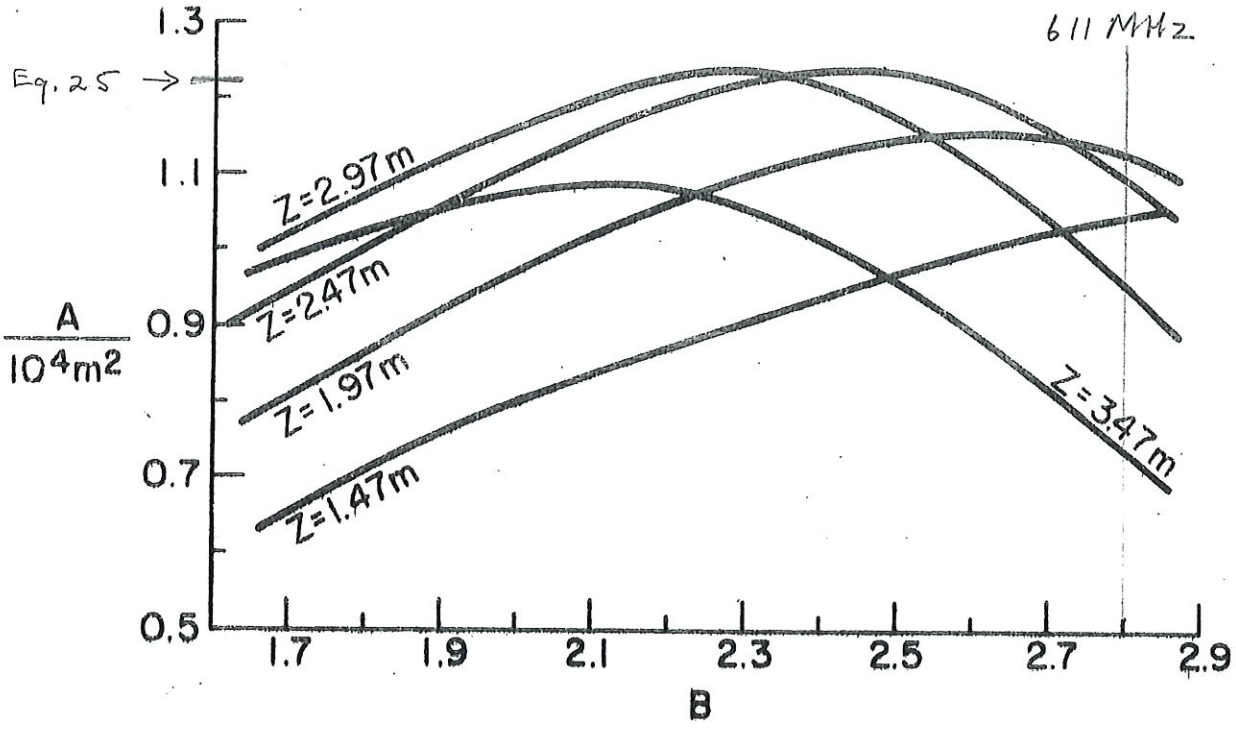

Figure 16

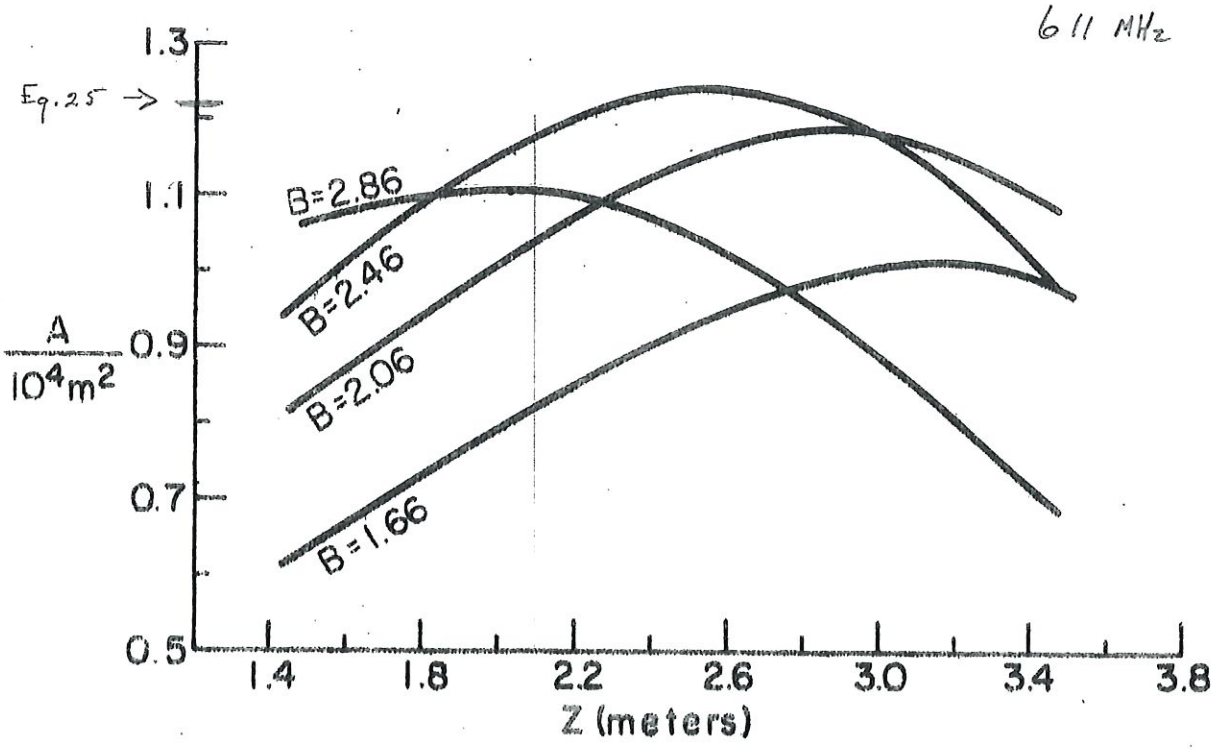

Figure 17

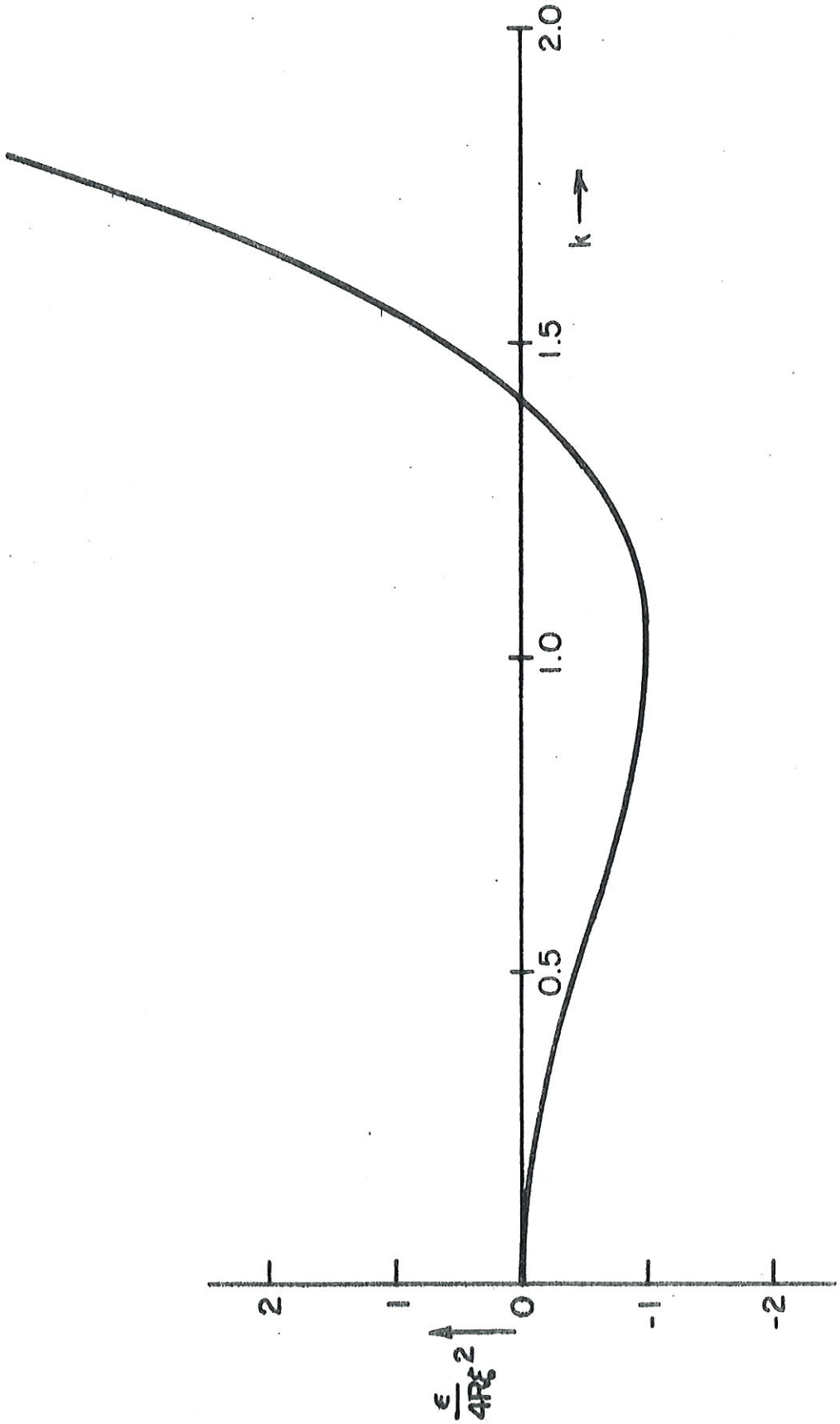

Figure 18

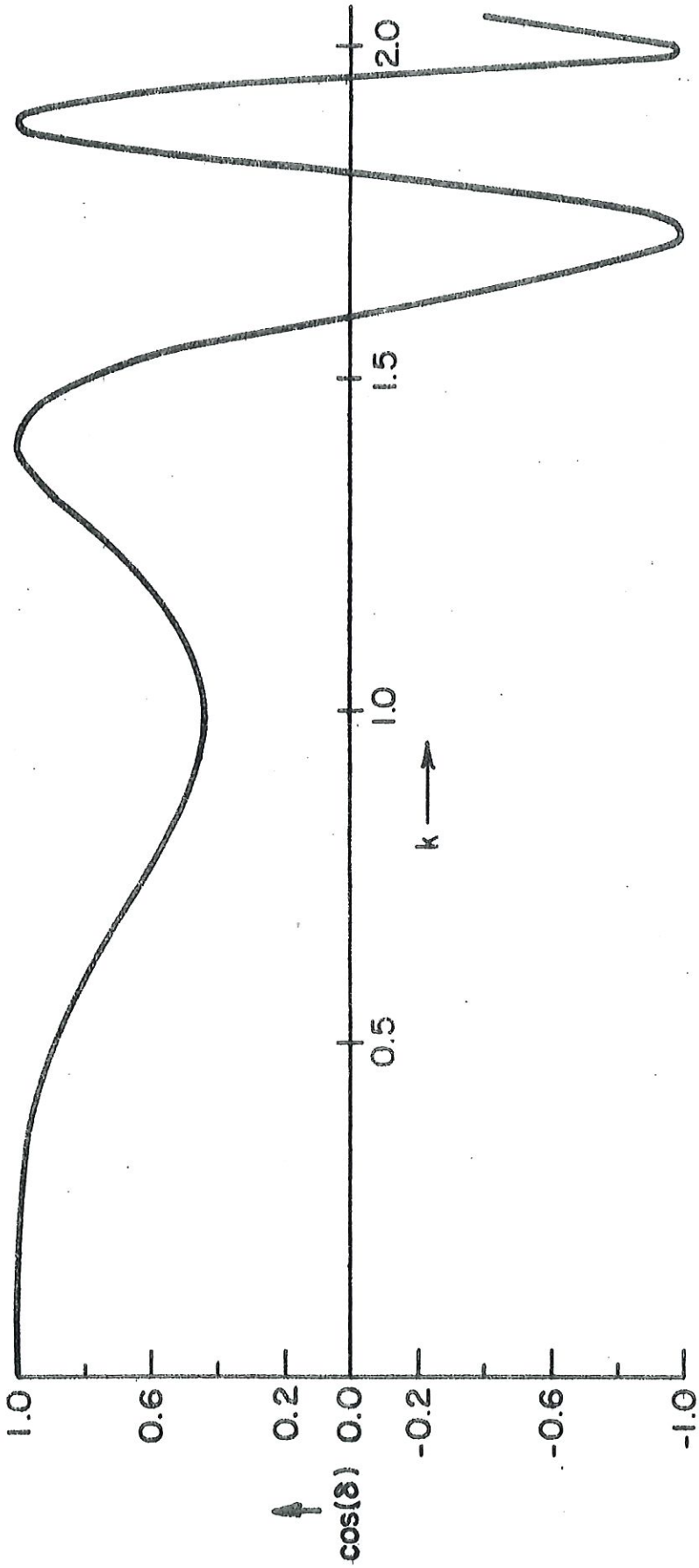

Figure 19

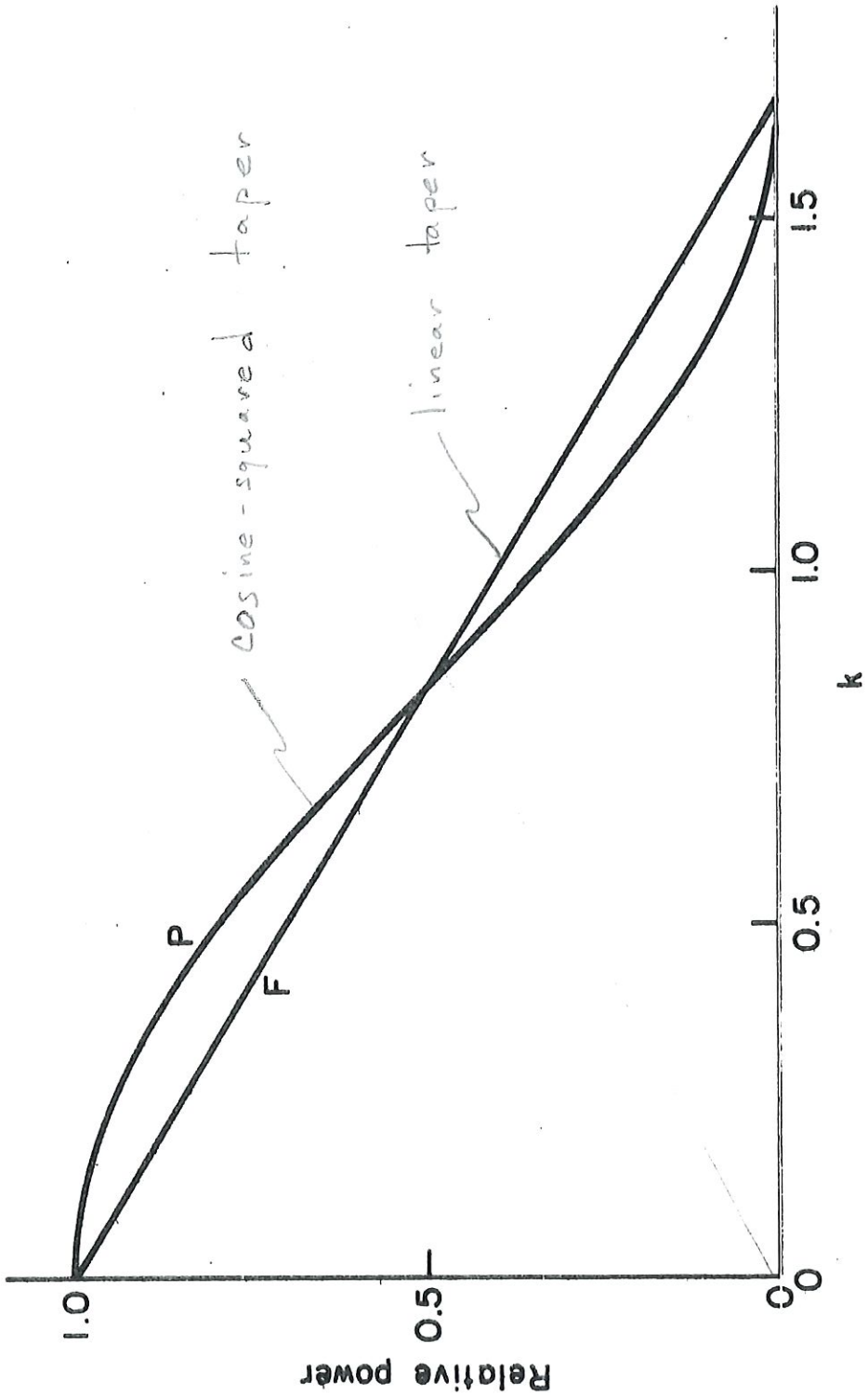
Relative power
1.0
0.5
0
0
0.5
1.0
1.5
k
P
F
cosine-squared taper
linear taper

Figure 20

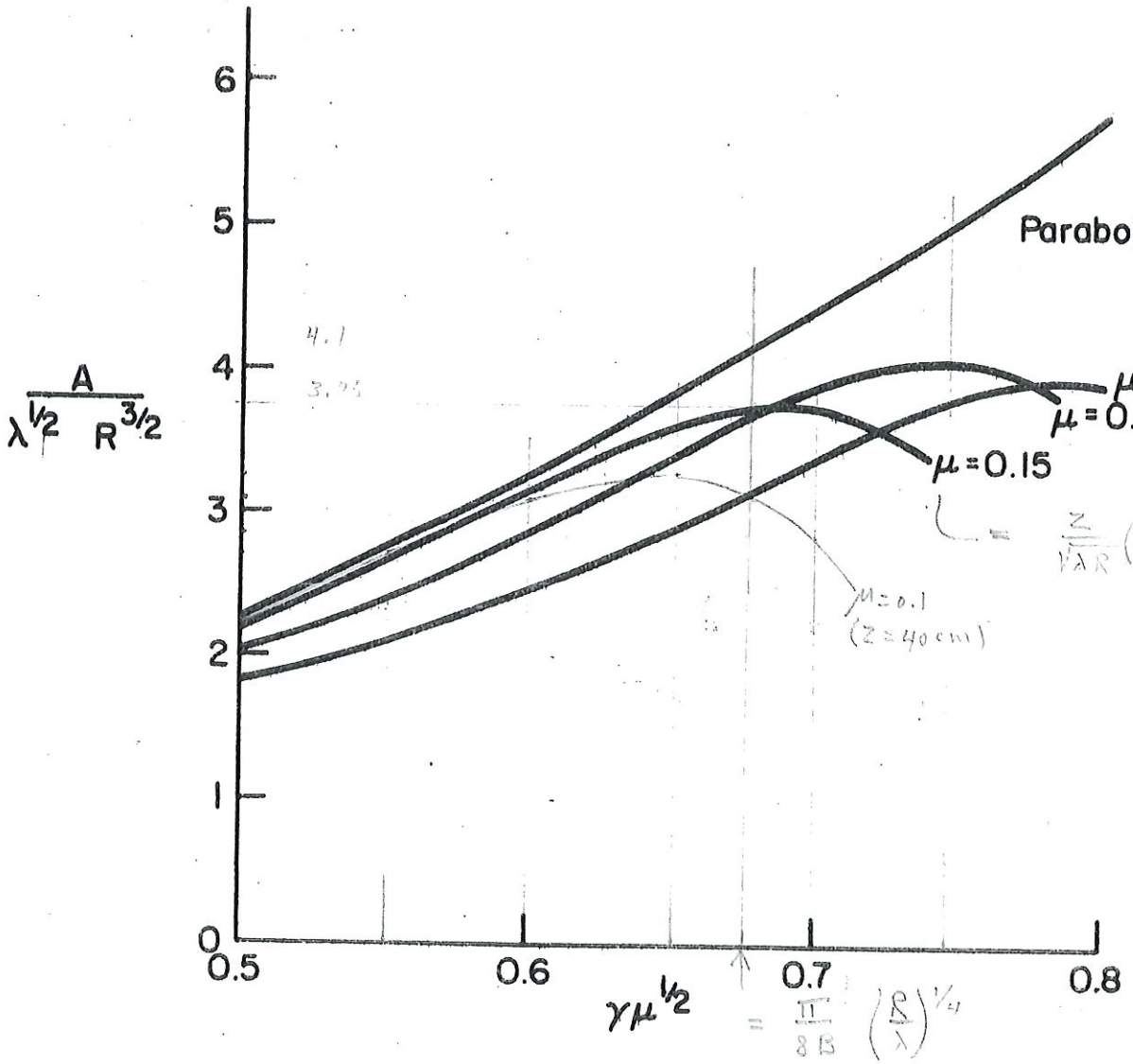
$\frac{A}{\lambda^{1/2} R^{3/2}}$
6
5
4
3
2
1
0
0.5
0.6
0.7
0.8
$\gamma\mu^{1/2}$
Paraboloid
$\mu = 0.25$
$\mu = 0.21$
$\mu = 0.15$
$\mu = 0.1$
(Z = 40 cm)

Figure 21

APPENDIX I

If a line feed is skewed so that it does not lie along a radius of the reflector which it illuminates, then both the form and position of the secondary pattern which they produce are changed. In this appendix we consider the effects of skewing a line feed of length t_o so that its lower tip is displaced a small distance x_o from the radius through its top. The primary field pattern F(r) is taken to be circularly symmetric so that any small segment of the line feed uniformly illuminates a ring on the reflector. The relation between the distance t of the segment below the paraxial surface and the radius r of the ring which it illuminates is (LaLonde and Harris 1970)

$$\sqrt{1 - r^2/R^2} = \frac{1}{(1 + \frac{2t}{R})}$$

where R is the spherical radius of the reflector. If ψ is the angle between the two radii passing through the top of the feed and through a point a distance t from the top, then, by geometry

$$\psi(t) = \frac{\frac{x_o}{t_o} t}{\frac{R}{2} + t}$$

so

$$\psi(r) = (\frac{x_o}{t_o}) \quad (1 - \sqrt{1 - \frac{r^2}{R^2}})$$

The polar field pattern $E(\phi)$ produced by a uniformly illuminated ring of radius r and width dr is

$$E(\phi) = \frac{2\pi}{\lambda^2} J_o \left(\frac{2\pi r \sin\phi}{\lambda}\right) dr$$

The power pattern produced by a skewed line feed is thus

$$P(\phi) = \left| \frac{2\pi}{\lambda^2} \int_0^\infty F(r) J_o \left(\frac{2\pi r \sin(\phi+\psi(r))}{\lambda}\right) dr \right|^2$$

This integral was evaluated numerically for a simple approximation to the illumination taper $F(r)$ of the 606 MHz line feed (LaLonde, private communication). The effects of skewing on forward gain and position are given approximately by equations A1 and A2 below.

$$\Delta\phi = 3.3\, x_o \qquad \text{(A1)}$$

$$G/G_o = 1 - (x_o)^2/20 = 1 - \frac{(x_2)^2 \times (4)^2}{20} \qquad \text{(A2)}$$

$$= 1 - (x_2)^2 \times .13$$

where $\Delta\phi$ = position shift in arc minutes

G/G_o = relative gain

x_o = displacement of feed tip in feet